

# Near-electrode and transient processes in liquid dielectrics

A I Zhakin

DOI: 10.1070/PU2006v049n03ABEH002012

## Contents

|  |            |
|--|------------|
| <b>1. Introduction</b>   | <b>275</b> |
| <b>2. Statement of the problem</b>   | <b>277</b> |
| <b>3. Structure of nonequilibrium layers</b>   | <b>279</b> |
| <b>4. Structure of the diffusion layer</b>   | <b>280</b> |
| <b>5. Kinetics of the elementary act</b>   | <b>281</b> |
| 5.1 Current situation; 5.2 Surface electronic states; 5.3 Population of surface states; 5.4 Effect of an external electric field; 5.5 Electron transition rate |            |
| <b>6. Analysis of transient processes</b>  | <b>290</b> |
| 6.1 Transition of dissociation – recombination reactions to equilibrium; 6.2 Time of ion wave travel; 6.3 Near-electrode transient processes                   |            |
| <b>7. Conclusions</b>  | <b>292</b> |
| <b>References</b>  | <b>294</b> |

**Abstract.** Electron transfer kinetics between an electrode and an electron acceptor in electrolytes, liquid dielectrics, and dense gases is comparatively analyzed for the case of a weak electric field. Near-electrode charge distribution patterns in a liquid dielectric (or a dense weakly conducting gas) exposed to an external high-voltage field are examined. It is shown that the quadratic dependence of current – voltage characteristics of the system is determined by the character of electron transitions from surface states. The transient processes involved are discussed, and characteristic formation times for steady-state near-electrode patterns are calculated.

## 1. Introduction

The main sources of free charges generated in a liquid dielectric are (1) dissociative decomposition of ion complexes (ion pairs and triplets [1–13]), and (2) various physical–chemical processes at the electrode–liquid interface, such as electrode dissolution (corrosion) [14], redox processes involving electron transfer reactions [3, 4, 9, 15–20], and some others [21–24].

The generation of surface charges in liquid dielectrics has important practical implications largely for two reasons.

(1) One is related to the development of effective injection electrodes. This problem in turn is subdivided into two cases including development of sharp and nonsharp electrodes.

The first case is especially difficult to address because an excessively high-strength field induced near a tip of the pin triggers rather complicated processes (molecular disintegration and polymerization [25], gas release [9, 10, 13, 26], electrode destruction due to microexplosions of microscopic inhomogeneities [21, 27, 28], cold electron emission, etc.). In effect this gives rise to a prebreakdown state near the microtip, frequently called the ‘corona’ [29, 30].

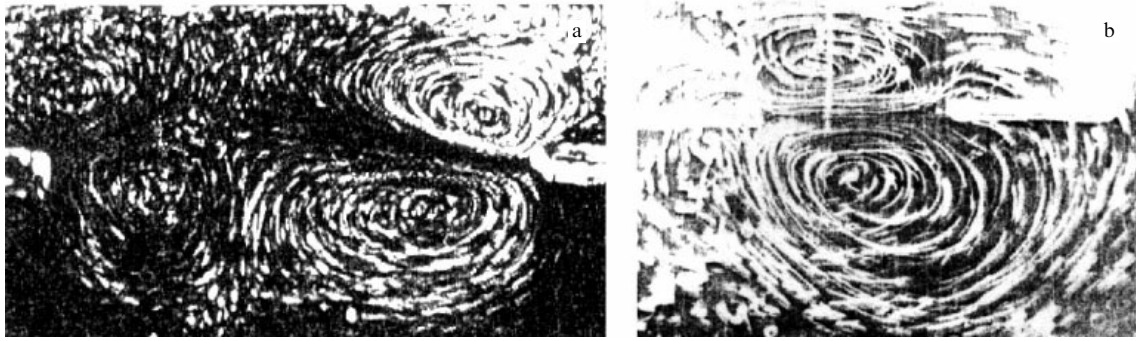
The results of experiments with slightly bent or flat electrodes suggest the leading role of redox processes in the ionization of liquids. By way of example, in a symmetric system of two parallel copper wires imbedded in transformer oil containing a polar admixture (butyl alcohol or aromatic hydrocarbons like iodobenzene and so on), the liquid flow consists of four eddies; in contrast, when molecular iodine is used as an admixture, only two eddies are formed and the flow is directed along the symmetry line from the cathode to the anode, as shown in Fig. 1 (see also Ref. [31]). These experiments indicate that polar liquids are characterized by bipolar electrochemical charge injection, as distinct from the unipolar injection of negative charges from the cathode that takes place in iodine solutions.

Different models of electrochemical injection are discussed in Refs [19, 20, 32]; one more important class of unipolar charge injection from ionite membranes into polar liquids in the absence of electron transfer reactions is considered in Ref. [33].

(2) Another important problem lies in electrochemical purification of liquids from ion impurities. For example, in the case of steady-state electroconvection of a dielectric liquid, charges injected by the emitter must be neutralized (discharged) at the collector. From the electrochemical point of view, liquid dielectrics constitute weak electrolytes with an incomplete dissociation of a salt dissolved into ion complexes: ion pairs, triplets, etc. [2, 8]. This view is in apparent conflict with the aqueous electrolyte theory that implies complete dissociation of salts. As an example, the double electric layer

A I Zhakin Kursk State Technical University,  
ul. 50-letiya Oktyabrya 94, 305040 Kursk, Russian Federation  
Tel. (7-4712) 504 795  
Fax (7-4712) 561 885  
E-mail: zhakin@mail.ru

Received 30 June 2004, revised 31 October 2005  
*Uspekhi Fizicheskikh Nauk* 176 (3) 289–310 (2006)  
Translated by Yu V Morozov; edited by A Radzig



**Figure 1.** Liquid flow patterns in a system of two parallel wires embedded in a transformer oil solution containing iodobenzene (a), and iodine (b). (Taken from Ref. [34]).

(DEL) thickness in aqueous solutions is given by the Debye radius, whereas in liquid dielectrics in the presence of a high-voltage [at least  $\geq 100 \text{ V cm}^{-1}$ ] electric field it is estimated [20, 32] as

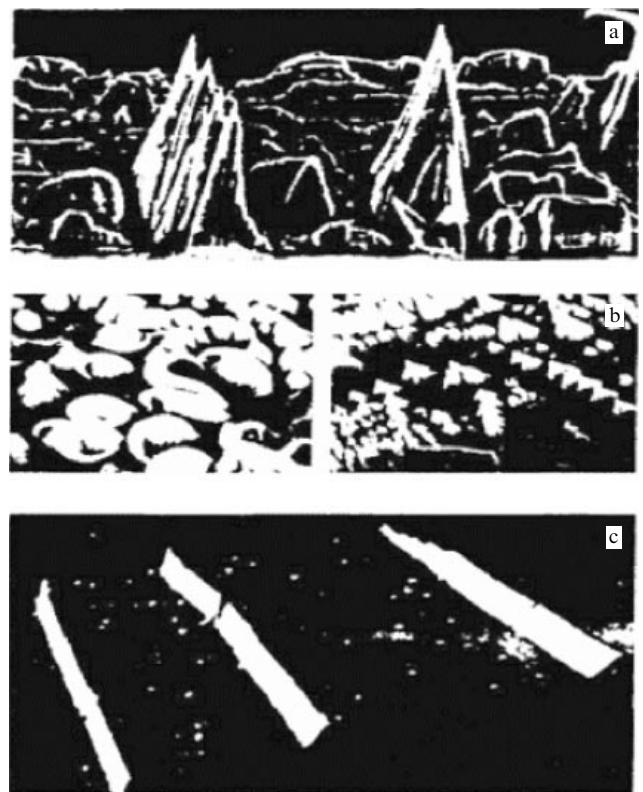
$$\xi_D = \frac{\varphi_0}{E_V}, \quad (1)$$

where  $\varphi_0 = k_B T/e$  is the specific osmotic potential equalling  $\varphi_0 = 0.026 \text{ V}$  at room temperature ( $k_B$  is the Boltzmann constant,  $T$  is the absolute temperature, and  $e$  is the proton charge), and  $E_V$  is the electric field strength on the outer side of the DEL. Because DEL properties are essentially different in aqueous and nonaqueous media, there is every reason to regard the latter as containing a simple diffusion layer.

Electrophysical processes at the interface between two media cannot be understood if the structure of the real surface is disregarded. Simplified models no longer predominate in the physics of semiconducting surfaces [35]; the same is true of the physics of high-voltage phenomena [21, 27, 28]. The real surface of any solid is far from being strictly flat; this is easily evidenced by having a look at an enlarged image of a surface thoroughly polished either mechanically [28] or by ion bombardment (Fig. 2a, b).

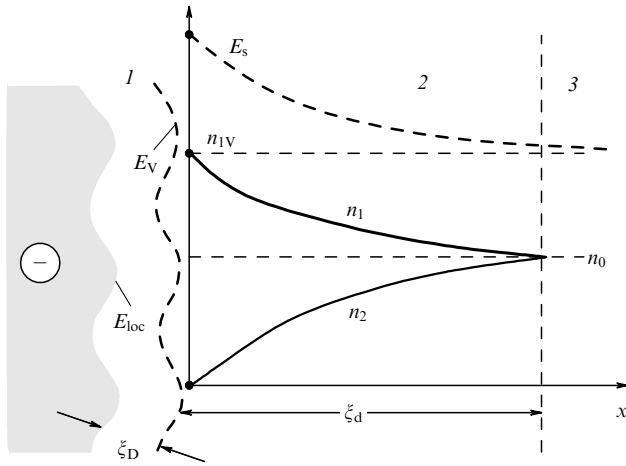
Only small regions of a surface may be arbitrarily regarded as flat provided they have been treated by special techniques (Fig. 2c). In strong electric fields, an important role is played by microtips at which the field increases by a factor of  $10^2 - 10^3$  [27, 28], so that the strength  $E_V$  is related to the so-called mean field  $E_s$  at the electrode by the expression  $E_V = \beta_s E_s$ , where  $\beta_s$  is the coefficient of field amplification by the microtip. According to Ref. [28],  $\beta_s = 10^2 - 10^3$ . Therefore, even in relatively weak fields,  $E_V \sim 1 \text{ kV cm}^{-1}$ , the diffusion layer thickness is  $\xi_D < 10^{-2} \text{ }\mu\text{m}$ , i.e., significantly smaller than the average linear dimensions of microtips. Following this line of reasoning, the electrode charge distribution near a surface can be schematically represented as shown in Fig. 3 [32].

Calculations of charge distribution in the near-electrode region taking into account the surface roughness were first done in Refs [20, 32]. The following features were revealed: (1) the near-electrode region consists of two layers — the diffusion layer, and the zone of nonequilibrium dissociation – recombination reactions (see Fig. 3); (2) the thickness of both layers,  $\xi_D$  and  $\xi_d$ , is essentially dependent on the external field strength [see formula (1) and Section 3], and (3) the local field strength  $E_{loc}$  near a microtip depends on the field strength  $E_V$  on the outer side of the diffusion layer and is given by the expression  $E_{loc} = \beta_D E_V$ , where  $\beta_D$  is the coefficient of amplification due to charges in the diffusion layer.



**Figure 2.** (a, b) Photographs of the surface of a copper single crystal following its treatment by ions at different angles ( $10^4\times$  magnification). (c) Photograph of a  $560 \times 50 \text{ nm}$  portion of the same surface after its special treatment.

It should be recognized that, despite the approval of the detailed analysis performed in Refs [20, 32] by interested researchers [19], it is not yet widely used, probably because of its excessive mathematical complication. There are numerous experiments and relevant calculations based on very simple models, the results of which are in good agreement with experimental data. However, an important drawback to this theoretical approach is the introduction of physically obscure phenomenological coefficients that are almost invariably assumed to be constant and actually found from experiment. For this reason, such theories have no predictive value in the general case. This dictates the necessity of developing a theory of microscopic processes at the metal – liquid dielectric interface, at least in the low-voltage ( $\sim 1 \text{ kV cm}^{-1}$ ) field region.



**Figure 3.** The structure of charged layers in the near-electrode region: 1 — diffusion layer, 2 — nonequilibrium layer, 3 — domain of the equilibrium dissociation–recombination reaction.

This paper is concerned with new approaches to the theory of electric conductivity of liquid dielectrics and, in fact, continues to develop the ideas put forward in a series of previous publications [8, 20, 32, 35]. Special attention is given to assessing the dependence of phenomenological parameters (e.g., rate constants of redox reactions) on external ones (e.g., electric field strength) based on detailing microscopic processes. In particular, it is shown that weakly bound electrode surface states play a leading role in contact electrization of liquid dielectrics and dense gases in the weak field region. Also considered are the charge and electric field strength distribution patterns in the near-electrode region with reference to dissociation–recombination reactions and the transient processes that determine the characteristic formation times of charged-containing structures. A method is discussed by which to measure parameters of contact processes, developed on the basis of the results of theoretical studies. Close attention is drawn to the investigations into contact processes in liquid dielectrics. It should be emphasized that electrization through the redox mechanism occurs in any weakly conducting medium, such as air or water. This accounts for the secondary objective of the present paper, namely, the assessment of the possibility of extending the available data to gases and electrolytes.

## 2. Statement of the problem

It is generally accepted that the conductivity of a liquid dielectric in the low-voltage region (see Section 3 for the definition) is determined by the presence of impurity ions  $A^+$  and  $B^+$  formed in the bulk due to the incomplete dissociation of a salt dissolved in the liquid in the form of ion pairs  $A^+B^-$  [1, 2, 7, 8]:



where  $k_d$  is the dissociation rate constant of ion pairs, and  $\alpha_{11}$  is the pair recombination coefficient of monoions  $A^+$ ,  $B^-$ .

A comprehensive analysis of conduction ion generation in the course of dissociation was presented in the review article [8] together with relevant examples of the corresponding

reactions; therefore, no special analysis of dissociative conductivity is made in the present paper.

Another type of charge generation in liquid dielectrics is associated with contact processes at the surface of the electrodes. It is, in turn, governed by several mechanisms including electrochemical injection [15–20, 32], desorption of physically adsorbed charges [36], cold emission of electrons from the cathode [9, 10, 13] and other specific physical injection mechanisms (acting in thin films [9, 21, 22] or in the case of microtip microexplosions in superhigh electric fields [21, 27]), and, finally, charge injection from ionite membranes into a polar liquid [33].

Most of these processes can be described mathematically by specifying boundary conditions at the injector for the number density of the charges being injected in the form [32, 35]

$$n_i = n_i(E), \quad (3)$$

where  $n_i(E)$  is the known function of the mean field  $E = E_s$  at the injector.

Functions  $n_i(E)$  are referred to as injection functions [35] although this term is not yet widely accepted. It should be borne in mind that the character of injection depends on the local field  $E_{loc}$ , the passage from which to the mean field is far from trivial (see Section 4).

An example is the form of an injection function of the reducing reaction of an electron acceptor  $X$  at the cathode:



where  $k_{X1}$  ( $k_{X2}$ ) is the rate constant of a direct (reverse) reaction.

Taking into consideration image forces, ion diffusion, and ion migration, it is possible to find that [20, 32]

$$n_i = \frac{k_{X1}c_X}{\mu E_{loc} + k_{X2}G(E_{loc})}, \quad (5)$$

where

$$G(E_{loc}) = \frac{eE_{loc}}{k_B T} \int_{r_0}^{\infty} \frac{g(x)}{g(r_0)} dx,$$

$$g(x) = \exp\left(\frac{\Pi(x)}{k_B T}\right), \quad \Pi(x) = -eE_{loc}x + \Pi_i(x).$$

Here,  $\mu$  is the mobility of  $X^-$  ions,  $c_X$  is the concentration of neutrals  $X$  at the electrode surface,  $r_0$  is the effective size of  $X^-$  ions, and  $\Pi_i(x) = -e^2/(16\pi\epsilon\epsilon_0 x)$  is the image force potential.

Relation (5) actually describes two processes, namely, the transfer of electrons to the adsorbed electron acceptor  $X$ , and the subsequent activation transfer of an  $X^-$  ion from the physical adsorption zone of the electrode surface to the bulk of the liquid under the action of the external electric field. Assuming that  $\mu E_{loc} \ll k_{X2}G(E_{loc})$ , Eqn (5) yields the injection function of physically adsorbed charges on the metal surface [36]:

$$n_i = \frac{n_0}{G(E_{loc})}, \quad (6)$$

where  $n_0 = k_{X1}c_X/k_{X2}$  is the constant concentration of adsorbed ions.

It is worth noting that the function  $G(E_{\text{loc}})$  for point ions ( $r_0 \rightarrow 0$ ) is transformed to the modified zero-order Bessel function  $G(E_{\text{loc}}) \rightarrow I_0(E_{\text{loc}})$  characterized by exponential asymptotics in the strong field region. In this case, relationship (6) takes the form of a classical expression describing the so-called Shottky injection [9, 10, 13, 36].

When charges are injected from an ionite membrane into a polar liquid, the membrane concentration of ions being injected is assumed to be constant and the injection itself is called autonomous [16, 17, 19, 33]. The calculation of electron transfer rate constants  $k_{X1}$ ,  $k_{X2}$  is an extremely difficult task due to, first, the lack of information on the real surface structure (the presence of defects, roughness, films, etc.), and, second, the necessity of taking into account effects of the double electric (diffusion) layer, the structure of which is in the general case unknown.

The most widely used are single-ion, two-ion, and three-ion conductivity models. The single-ion model fairly well describes the conductivity of polar dielectrics in the case of strong unipolar charge injection from the membrane [33]. The two-ion model is applied to the description of the low-voltage impurity conductivity of any dielectric because, in this case, charges are generated only in the course of a dissociation reaction (2). Finally, the three-ion model is in satisfactory agreement with experiment in the presence of both dissociative conductivity [due to reaction (2)] and charge injection induced, for example, by reaction (4).

Evidently, the three-ion model is the most general one; it transforms into the two-ion dissociation–injection model in the presence of weak fields, and to the single-ion model of unipolar injection conductivity in the presence of strong electric fields [35]. For this reason, the three-ion model is regarded as a basic one. Thus, the principal equations of current transfer (disregarding liquid movements) have the form

$$\text{div}(\varepsilon \varepsilon_0 \mathbf{E}) = e(n_1 - n_2 - n_4), \quad \mathbf{E} = -\nabla \varphi, \quad (7)$$

$$\frac{\partial n_j}{\partial t} + (-1)^{j-1} \text{div}(\mu_j n_j \mathbf{E}) = \dot{\xi}_j, \quad j = 1, 2, 4; \quad (8)$$

$$\dot{\xi}_1 = \dot{\xi}_2 + \dot{\xi}_4, \quad \dot{\xi}_2 = k_d N - \alpha_{11} n_1 n_2, \quad \dot{\xi}_4 = -\alpha_{11} n_1 n_4.$$

Here,  $\varepsilon$  is the relative permittivity of the liquid,  $\varepsilon_0$  is the electric constant,  $n_1, n_2, n_4$  are the bulk concentrations of  $A^+$ ,  $B^-$ ,  $X^-$  ions,  $\mu_1, \mu_2, \mu_4$  are their respective mobilities,  $N$  is the concentration of ion pairs  $A^+B^-$  assumed to be constant [8],  $\alpha_{11}$  is the pair recombination coefficient for  $A^+$  and  $X^-$  ions, and  $\varphi$  is the electric field potential.

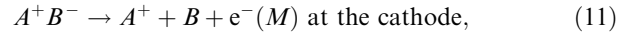
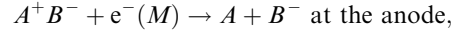
Equations (7), (8) should be considered in terms of mechanics of continuous media, which means that all quantities in them are the averages taken over a physically small but finite volume. Therefore, the boundary conditions for Eqns (7), (8) must have the same sense, i.e., be specified at averaged ‘smooth’ surfaces. As appears from Fig. 3, this fact implies that these boundary conditions must be set on a smooth surface  $S$  separated from the real one by a distance equalling approximately a few characteristic sizes of surface microtips. In fact, the boundary conditions are specified by setting the interelectrode potential difference  $U$  (the voltage drop inside the diffusion layers usually being small) and the nonflow condition for  $A^+$  ions at the anode:

$$\varphi = U, \quad n_1 = 0, \quad (9)$$

and also by setting the nonflow condition for  $B^-$  ions and the injection function of  $X^-$  ions at the cathode:

$$\varphi = 0, \quad n_2 = 0, \quad n_4 = n_i(E). \quad (10)$$

Strictly speaking,  $A^+$ ,  $B^-$  impurity ions may also be formed at the electrodes, for example, due to the neutralization of one of the members of pair  $A^+B^-$  in the following reactions [19, 32]:



where  $e^-(M)$  stands for an electron passing to the electrode (from the electrode).

That processes (11) actually take place is confirmed not only by the estimates of their activation energies but also by experimental data. For example, the flow from a pin electrode in liquid dielectrics is observed at both positive and negative polarity of the pin [29–31, 37]. The results of simple estimations indicate that only a very small fraction of ion pairs is subject to reduction (oxidation). It was shown in Ref. [8] that the concentration of ion pairs even in well-purified nonpolar dielectrics does not fall below  $10^{17} \text{ cm}^{-3}$ , whereas the typical concentration of the injected ions is on the order of  $10^{12} \text{ cm}^{-3}$ . These processes are supposed to be especially intense at pin electrodes and much less so at slightly bent ones. The detailed microscopic mechanism of such injection is poorly known [19] and needs special consideration in both theoretical and experimental contexts.

The second type of equations and boundary conditions is of a microscopic character and describes the field and charge distributions in a diffusion layer. In essence, these equations were deduced for one-particle distribution functions of ions. Dissociation and recombination processes inside a thin diffusion layer may be neglected, but it is necessary to take into account the effects of short-range forces induced by the electrode surface. Let us consider a system of equations describing the distribution of  $A^+$  ions in the cathode diffusion layer in the absence of the injection of  $B^-$  and  $X^-$  ions. The introduction of an  $x$ -coordinate normal to the electrode surface yields

$$\varepsilon \varepsilon_0 \frac{\partial E_x}{\partial x} = en_1, \quad \frac{\partial n_1}{\partial t} + \frac{\partial i_{1x}}{\partial x} = 0, \quad (12)$$

$$i_{1x} = -D_1 \frac{\partial n_1}{\partial x} + \mu_1 n_1 E_x + \frac{\mu_1}{e} n_1 f_{1x},$$

where  $E_x$ ,  $f_{1x}$  are the  $x$ -components of the electric field strength and the short-range force, respectively, and  $D_1$  is the diffusion coefficient. The boundary conditions can be formulated without loss of generality for an ion neutralization reaction in the form



where  $k_{A1}$  ( $k_{A2}$ ) is the rate constant of direct (inverse) electron transfer. Taking into consideration chemical kinetics propositions and current continuity conditions on the outer side of the diffusion layer, the boundary conditions can be written

down as

$$k_{A1}n_1(r_0) - k_{A2}c_A = i_1 \quad \text{at } x = r_0, \quad (14)$$

$$E_x = -E_V, \quad n_1 = n_{1V} \quad \text{at } x = \xi_D, \quad (15)$$

where  $i_1$  is the migration current of  $A^+$  ions,  $E_V$ ,  $n_{1V}$  are the field strength and the number density of  $A^+$  ions on the outer side of the diffusion layer, which are found from the external problem (see Section 4),  $\xi_D$  is the unknown thickness of the diffusion layer to be determined, and  $c_A$  is the product  $A$  concentration at the electrode surface.

The problem stated by Eqns (12), (14), (15) constitutes the basis for the computation of  $\beta_D$ ,  $\xi_D$  and the characteristic formation time of steady-state near-electrode charge distribution patterns.

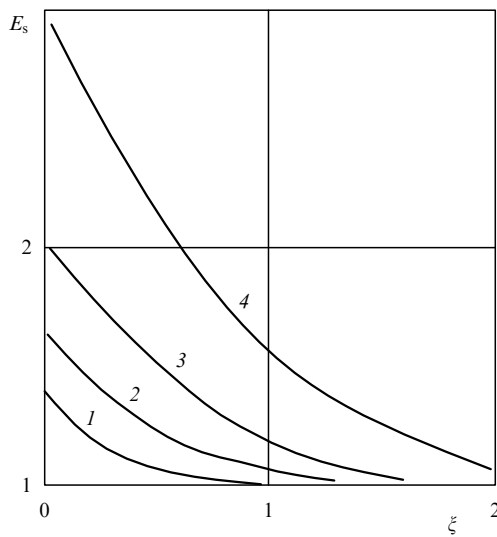
### 3. Structure of nonequilibrium layers

We shall start with the consideration of stationary near-electrode structures in the weak field region when charge injection is insignificant. This means that  $n_4 = 0$  and ohmic conductivity is determined by the coefficient  $\sigma = e(\mu_1 + \mu_2)n_0$ , where  $n_0 = \sqrt{k_d N / \alpha_{11}}$  is the equilibrium concentration of  $A^+$ ,  $B^-$  ions far from the electrodes. Because positive (negative) ions near the anode (cathode) are 'drawn off' the electrode, the equilibrium of the dissociation–recombination reaction (2) is disturbed. This results in the formation of nonequilibrium layers near the electrodes that have the thickness

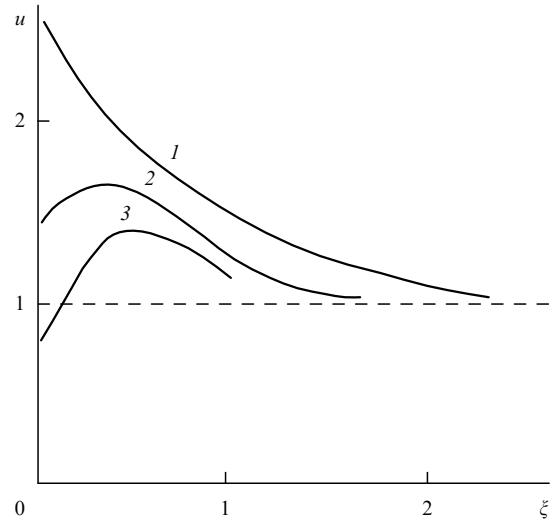
$$\xi_d \approx \frac{\varepsilon \varepsilon_0 E_0}{en_0} = \frac{\varepsilon \varepsilon_0 E_0 (\mu_1 + \mu_2)}{\sigma}, \quad (16)$$

where  $E_0$  is the electric field strength at the interface between the equilibrium and nonequilibrium zones (see Fig. 3).

Formation of nonequilibrium layers with a thickness defined by relationship (16) was first observed in studying an electrical conductivity of weakly conducting dense gases [38] and described again for liquid dielectrics in the absence of injection [35, 39–41] (see Fig. 4). Another structural type of near-electrode layers was discovered in an iodine-containing



**Figure 4.** Field distribution in a nonequilibrium layer at  $\sigma_A = f_A = 0$ ;  $\xi = x/\xi_d$ . Curve 1 corresponds to  $\beta_2 = 0.5$ , 2 —  $\beta_2 = 1.0$ , 3 —  $\beta_2 = 2.0$ , and 4 —  $\beta_2 = 5.0$ .



**Figure 5.** Distribution of the dimensionless field strength  $u(\xi)$  in the non-equilibrium near-electrode region ( $\xi = x/\xi_d$ ) at  $\beta_2 = 1$ ,  $\beta_4 = 0.2$ : 1 —  $\sigma_A = 0$ ; 2 —  $\sigma_A = 4$ , and 3 —  $\sigma_A = 10$ .

transformer oil solution around copper electrodes [42]. As noted in Section 2, the cathode in such a solution is the site of a reducing reaction giving rise to negative ions (electrochemical injection). Under these conditions, so-called bipolarly charged layers may form, with the charge of the layer adjacent to the electrode having the sign corresponding to electrode polarity (see Fig. 5). Physical mechanisms underlying the formation of such structures are rather simple: when the mobility of the ions being injected is low, the zone of their recombination with heteroions is displaced toward the interior of the nonequilibrium layer; as a result, the near-electrode zone is enriched with injected homoions, while the region adjoining the liquid becomes rich in heteroions. The existence of these layers is apparent from the vibrational motion of a small dispersed particle (the size of which is commensurate with the thickness of the nonequilibrium zone) near the electrode. The particle vibration is due to its recharging as it alternately enters oppositely charged layers; the result is the altered direction of the Coulomb force action. It follows from relationship (16) that the thickness of the nonequilibrium layer linearly increases with increased field strength. However, the size of the nonequilibrium region grows much faster in the presence of injection. For this reason, the homocharged zone in sufficiently strong fields spreads over the entire interelectrode gap and unipolar injection conductivity sets in [35].

A few estimates are in order. At typical values of  $E_0 = 100 \text{ kV m}^{-1}$ ,  $\mu_1 \sim \mu_2 \sim 10^{-8} \text{ m}^2 \text{ V}^{-1} \text{ s}^{-1}$ ,  $\sigma \sim 10^{-11} \text{ } \Omega^{-1} \text{ m}^{-1}$ , and  $\varepsilon \sim 2$ , it follows from formula (16) that  $\xi_d = 0.2 \text{ mm}$ . Therefore, the near-electrode nonequilibrium layers have a macroscopic size and can be well observed using routine experimental procedures (e.g., probe method, as described in Ref. [42]).

In what follows, we briefly dwell on the method and the results of theoretical studies on the structure of non-equilibrium layers in the general case. For certainty, let us consider the cathode.

The field and charge distribution patterns are expressed by

$$E_x = -u(\xi) E_0, \quad n_j = p_j(\xi) n_0, \quad (17)$$

where  $u(\xi)$ ,  $p_j(\xi)$  are the universal functions defined as the solution of the following boundary value problem:

$$\begin{aligned} -\frac{du}{d\xi} &= p_1 - p_2 - \sigma_A p_4, \quad (-1)^j \frac{d(\beta_j p_j u)}{d\xi} = \Sigma_j, \\ \Sigma_1 &= \Sigma_2 - \sigma_A(1 + \beta_4) p_1 p_4, \quad \Sigma_2 = (1 + \beta_2)(1 - p_1 p_2), \\ \Sigma_4 &= -(1 + \beta_4) p_1 p_4; \\ \beta_j &= \frac{\mu_j}{\mu_1}, \quad j = 1, 2, 4; \quad \sigma_A = \frac{n_i(E_0)}{n_0}; \\ \xi = 0: \quad p_4 &= f_A \equiv \frac{n_i(E)}{n_i(E_0)}, \quad p_2 = 0; \\ \xi \gg 1: \quad u &\rightarrow 1, \quad p_1 \rightarrow 1, \end{aligned} \quad (18)$$

where  $\xi = x/\xi_d$ ,  $x$  is the coordinate normal to the electrode surface, having the origin at the cathode and directed into the depths of the liquid, and  $u = -E_x/E_0$ ,  $p_j = n_j/n_0$ .

The results of analytical and numerical studies [43] of problem (18) revealed the following features.

In the absence of injection ( $\sigma_A = f_A = 0$ ), function  $u$  depends only on the ratio  $\beta_2 = \mu_2/\mu_1$  between mobilities:  $u = u(\xi, \beta_2)$ . The values of function  $u$  increase with growing mobility of homoions (ions with the sign identical to the electrode polarity); in other words, the near-electrode field becomes progressively stronger (see Fig. 4). The mobility of positive ions being normally higher than that of negative ones [8–10], the field in the vicinity of the anode must be stronger as well (given the plane geometry of electrodes). The non-equilibrium layers are enriched in heteroions, and the near-electrode layers acquire charges opposite in sign with respect to electrode polarity.

In the presence of injection, so-called bipolarly charged layers may form. In this case, the charge of the layer adjacent to the electrode is consistent with electrode polarity (see Fig. 5). As shown by computation [43], the formation of such structures is feasible under the following conditions: (1) the homoion injection level is sufficiently high [parameter  $\sigma_A \geq 1$  in problem (18)], and (2) the mobility of the ions being injected is lower than that of impurity ions [parameter  $\beta_4 < 1$  in problem (18)].

Furthermore, it follows from relationships (17) that quantities  $E_s \equiv E_x(0) = u(0)E_0 \equiv E_V$ ,  $n_{2s} = p_2(0)n_0 \equiv n_{2V}$  actually dictate both the field strength and the concentration of heteroions on the outer side of a diffusion layer (see Fig. 3). We should also note that the mean field  $E_s$  and the concentration  $n_{2V}$  of heteroions increase linearly with increasing field strength and impurity conductivity (at impurity concentration  $n_0$ ). In other words, a rise in ohmic conductivity leads to a decrease in the thickness of nonequilibrium layers, whereas peak field strengths increase. In practice, this regularity manifests itself in the dependence of the injection current on the impurity conductivity, which is frequently observed in experiment [37].

#### 4. Structure of the diffusion layer

It will be shown in this section that the diffusion layer consists of two sublayers: the adsorption one, and the diffusion layer proper. Let us compute analytical expressions for the field and charge distributions in each sublayer and use them to show that the local field  $E_{loc}$  at the electrode surface and the external field  $E_V$  on the outer side of the diffusion layer are

related as  $E_{loc} = \beta_D E_V$ , where  $\beta_D$  is the coefficient of field amplification by the diffusion layer ( $\beta_D > 1$ ). In what follows, we shall present analytical expressions for the surface charge  $q_s$  and capacitance  $C_s$  that can, in principle, be found experimentally. Charge  $q_s$  being inversely proportional to the ion neutralization (discharging) rate constant  $k_1$ , the measurement of  $q_s$  gives  $k_1$ .

For certainty, we shall consider the cathode diffusion layer. In a stationary case, Eqns (12) yield the equations

$$\begin{aligned} \varepsilon \varepsilon_0 \frac{dE_x}{dx} &= en_1, \\ -D_1 \frac{dn_1}{dx} + \mu_1 n_1 E_x + \frac{\mu_1}{e} n_1 f_{1x} &= -i_1 \equiv -\mu_1 n_{1V} E_V, \end{aligned} \quad (19)$$

for which the boundary conditions have the forms (14), (15).

Bearing in mind that the radius of action of the image force is considerably smaller than the thickness  $\xi_D$  of the diffusion layer, it is possible to distinguish two sublayers in the diffusion layer. One makes up the region of physically adsorbed charges, in which the short-range force is much greater than the Coulomb force:  $|f_{1x}| \gg e|E_x|$ . The other is the diffusion sublayer proper, in which the inverse inequality  $|f_{1x}| \ll e|E_x|$  is fulfilled.

For the adsorption sublayer, it follows from equation (19) that

$$n_1 = n_{1*} \exp\left(-\frac{\Pi_1(x)}{k_B T}\right), \quad (20)$$

where  $n_{1*}$  is the value of concentration  $n_1(x)$  at the adsorption sublayer border, i.e., at  $x = x_*$ ; the value of  $x_*$  may be found from the condition  $-\Pi_1(x_*) \approx k_B T$ ; hence, we arrive at

$$x_* \approx \frac{e^2}{16\pi \varepsilon \varepsilon_0 k_B T} \equiv \xi_{ad}. \quad (21)$$

For a nonpolar dielectric at  $\varepsilon \sim 2$  and  $T = 300$  K, one obtains  $\xi_{ad} \approx 100$  Å, or it is much smaller than typical values of the diffusion layer thickness  $\xi_D \geq 3 \times 10^3$  Å; this means that the above propositions are correct.

Within the diffusion sublayer  $\xi_{ad} \leq x \leq \xi_D$ , the system of equations (19) in the approximation of charge quasi-equilibrium distribution  $i_1 \ll \mu_1 n_1 |E_x|$  (which can also be written in the form of the easily verifiable criterion  $C_D \equiv en_{1V} \xi_D / (\varepsilon \varepsilon_0 E_V) \ll 1$ ) has the solution

$$E_x = -E_V \frac{1 + C_1 \exp(-\xi)}{1 - C_1 \exp(-\xi)}, \quad (22)$$

where

$$\begin{aligned} \xi &= \frac{x}{\xi_D}, \\ C_1 &= 1 + \frac{1}{C_*} - \sqrt{\left(1 + \frac{1}{C_*}\right)^2 - 1}, \quad C_* = \frac{en_{1*} \xi_D}{\varepsilon \varepsilon_0 E_V}. \end{aligned}$$

Thus,  $n_{1*}$  remains the sole undetermined parameter in both the solutions (20) and (22). It can be found using boundary condition (14):

$$\begin{aligned} n_{1*} &= \frac{n(r_0)}{K_{1A}} = \frac{i_1 + k_{A2} C_A}{K_{1A} k_{A1}}, \quad i_1 = \mu_1 n_{1V} E_V, \\ K_{1A} &= \exp\left(\frac{\xi_{ad}}{r_0}\right). \end{aligned} \quad (23)$$

Here,  $K_{1A}$  is the adsorption coefficient of  $A^+$  ions due to the action of image forces.

It follows from relationship (22) that the thickness of the diffusion layer is determined by the value of  $\xi_D$ . The amplification coefficient due to the diffusion sublayer can be found from formula (22) for  $\xi \rightarrow 0$ :

$$|E_x(0)| = \beta_{D2} E_V, \quad \beta_{D2} = \sqrt{1 + 2C_*}. \quad (24)$$

Taking into consideration formula (21), the field inside the adsorption sublayer  $r_0 \leq x \leq \xi_{ad}$  is defined as

$$E_x = -\frac{en_1^*}{\varepsilon\varepsilon_0} \int_x^{\xi_{ad}} \exp\left(\frac{\xi_{ad}}{x}\right) dx - \beta_{D2} E_V. \quad (25)$$

Hence, the final expressions for the local electric field  $E_{loc}$  and the amplification coefficient  $\beta_D$  are given by

$$E_{loc} = |E_x(r_0)| = \beta_D E_V, \quad \beta_D = \beta_{D1} + \beta_{D2}, \quad (26)$$

$$\beta_{D1} = \frac{en_1^*}{\varepsilon\varepsilon_0 E_V} \int_x^{\xi_{ad}} \exp\left(\frac{\xi_{ad}}{x}\right) dx, \quad \beta_{D2} = \sqrt{1 + 2C_*}.$$

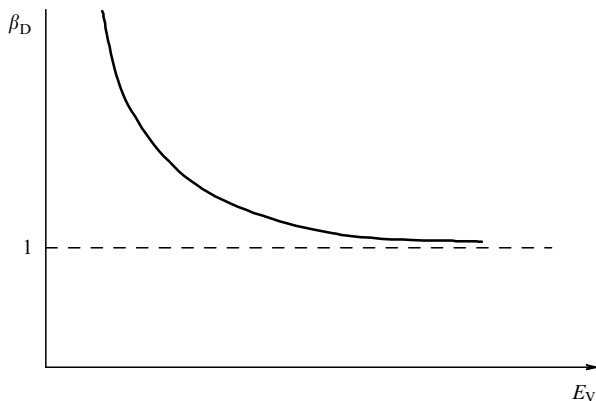
Relationships (26), taking into account formulas (22), (23), and the general field dependence of rate constants  $k_{A1}$ ,  $k_{A2}$  ( $k_{A1}$  exponentially grows, and  $k_{A2}$  exponentially decreases [19, 20]), lead to the conclusion that the coefficient  $\beta_D$  monotonically decreases as the external field becomes stronger, so that in strong fields  $\beta_D \rightarrow 1$ . The dependence of  $\beta_D$  on  $E_V$  is schematically presented in Fig. 6.

Although we have derived the analytical expression for the amplification coefficient  $\beta_D$  and found the form of its dependence on the external field, it is impossible to draw any conclusion as regards concrete numerical values of  $\beta_D$  for the lack of information on the discharging reaction rate constants  $k_{A1}$ ,  $k_{A2}$ . Nevertheless, the result obtained is of importance for the solution of the inverse problem, i.e., determination of reaction rate constants  $k_{A1}$ ,  $k_{A2}$  from the characteristics of the diffusion layer. Indeed, it is possible, using expressions (22), (25), to determine a voltage drop in the diffusion layer:

$$\Delta\varphi = \int_{r_0}^{\xi_D} E_x dx,$$

and the surface charge

$$q_s = e \int_{r_0}^{\xi_D} n_1 dx = \varepsilon\beta_D E_V, \quad (27)$$



**Figure 6.** Schematic of the dependence of amplification coefficient  $\beta_D$  on the external field.

from which the capacity of the diffusion layer is obtained at once:

$$C_s = \frac{q_s S}{\Delta\varphi},$$

where  $S$  is the electrode area.

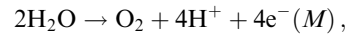
The value of  $q_s$  can be obtained by measuring characteristics of the transient process (see Section 6.3), and  $C_s$  from cell resistance in the alternating field. In principle, these data can also be used to find  $k_{A1}$ ,  $k_{A2}$  values.

## 5. Kinetics of the elementary act

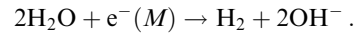
### 5.1 Current situation

Investigations into electron transitions at the solid–liquid (gas) interface are based on two approaches: physical [34, 44, 45], and electrochemical [46–51] that comprise, like the bulk conductivity theory [8], a variety of methods, ideas, terms, and propositions. Electrochemical kinetics is best developed for aqueous solutions and is based on the following premises:

(1) Electron transitions are called *redox reactions* or the *electrode process*. The main study areas include electrode processes of ion discharging, such as ion discharging on the cathode, exemplified by reaction (13). Due to the high chemical activity of water as a solvent, redox reactions can be very complicated. The simplest classification distinguishes between *reversible* (e.g., ion charge exchange) and *irreversible* reactions, the latter being the predominant processes, for example, water decomposition with the release of hydrogen ions at the anode:



and hydroxyl groups at the cathode:

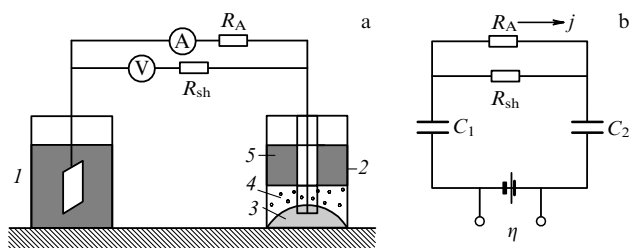


These processes proceed in relatively weak fields (mean field strength on the order of  $100 \text{ V cm}^{-1}$  in a flat capacitor).

Let us note that organic liquids (the predominant type of liquid dielectrics) are known to intensively absorb water. Suffice it to mention that the limiting solubilities of water in nonpolar benzene and in polar nitrobenzene are 0.163% and 0.19% at  $20^\circ\text{C}$ , respectively, if expressed as mass concentration (see [52, p. 692]); this is equivalent to  $\sim 10^{20} \text{ cm}^{-3}$  in volume concentration units. Bearing in mind that the typical bulk concentration of charges in liquid dielectrics equals  $10^{12} \text{ cm}^{-3}$ , it is easy to understand the role of water in the electroconductivity of technical liquid dielectrics and the related effects (e.g., electroconvection).

Moreover, the reactions are accompanied by structural changes in the surface of an electrode, such as its dissolution or, conversely, the release of reaction products on its surface (see Sections 5.1 and 5.2).

(2) The so-called *electrode potential*  $\eta$  is introduced. It is a specific quantity having nothing to do with the charge electric field potential.  $\eta$  is measured with a highly sensitive voltmeter as the potential difference between the electrode under consideration (the surface of which is the site of an electrochemical process) and the reference electrode (hydrogen or calomel [48]). The most frequently measured quantities are the electric current  $j$  as a function of  $\eta$  or its time



**Figure 7.** (a) Schematic of the experimental setup: 1 — cell involved, 2 — reference (calomel) electrode (3 — mercury, 4 — calomel  $\text{HgCl}_2$ , 5 — aqueous  $\text{HCl}$  solution). (b) Equivalent scheme:  $R_A$ ,  $R_{sh}$  — amperemeter and voltmeter shunt resistances;  $C_1$ ,  $C_2$  — DEL capacitances at the electrode under test and reference electrode.

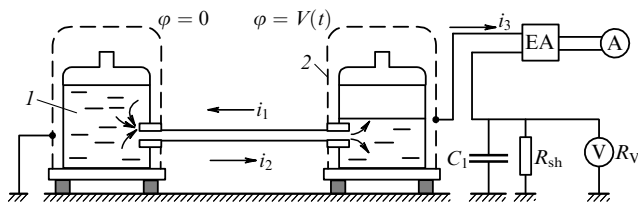
dependence  $j(t)$  as an ampere–time (AT) characteristic. A typical layout of the measuring setup is depicted in Fig. 7a, and its equivalent scheme in Fig. 7b. It is worth mentioning that ohmic resistance is usually neglected because of small DEL thicknesses.

When  $R_{sh} \gg R_A$ , the current flow in the circuit is described by the equation

$$\frac{d\eta}{dt} = R_A \frac{dj}{dt} + \left( \frac{1}{C_1} + \frac{1}{C_2} \right) j. \quad (28)$$

Quantities  $\eta(t)$ ,  $j(t)$  being measurable, this equation may be used to calculate DEL capacitance  $C_1$  at the electrode under test. Certainly, this experimental procedure should be employed with some reservation because capacitance  $C_1$  is in the general case a function of  $\eta$  [47, 48] and calculations with Eqn (28) give only estimates.

Additional information about the ion composition of a liquid is needed if kinetic characteristics of the electrode process are to be determined. For example, it is supposed that conductivity of weakly conducting media (air, liquid dielectrics, etc.) is due to monoions and ion complexes (ion pairs, triplets, etc. [8]) that can be detected only by additional measurements. This is especially important in the context of static electrization of organic liquids [53–59]. In this case, the approach to the study of contact processes is somewhat different from the method discussed earlier in this section. The typical experimental setup for this purpose is depicted in Fig. 8 [57]. Charges are supposed to be separated by two principal mechanisms at the tube surface in contact with the liquid. One of them consists in charge adsorption and the subsequent formation of a DEL whose diffusion component escapes with the liquid to the reservoir and charges it. The other mechanism is underlain by the electrode process. Studies reported in Ref. [57] demonstrated that adsorption mechanisms are responsible for electrization during the fluid



**Figure 8.** Schematic of the setup for liquid electrization studies [57]: 1 — liquid being studied, 2 — Faraday cell, EA — electrometric amplifier.

passage through a tube of dielectric material (Teflon), while redox mechanisms play a similar role in metal tubes.

Different standpoints are also worth mentioning. For example, it was suggested [55, 56] that electrization of liquids in metal tubes may also be governed by the adsorption mechanism.

Other electrochemical methods for the study of redox processes are reviewed in Ref. [60].

(3) Two main problems can be arbitrarily distinguished in electrochemical kinetics [48].

One is related to the explanation of charge acquisition by an electrode as it is embedded in an electrolyte solution. In electrochemistry, this phenomenon is referred to as electrode *polarization*. It is accepted that charging of a metal electrode occurs either as a result of ion transfer from the ionic skeleton of the metal to the solution (in which case the electrode acquires a negative charge) or, conversely, through the attachment of positive ions to the crystal lattice of the metal (with the electrode being charged positively). In the equilibrium case, this problem is resolved by the thermodynamic method — that is, by equating chemical potentials  $\mu^m$  of a positive ion in the metal (assuming that  $\mu^m = \text{const}$ ) and in the solution,  $\mu = \mu^0 + k_B T \ln c_i - e\varphi$ , where  $c_i$  is the ion concentration, and  $\varphi$  is the electrostatic field potential created by ions and the charged electrode. Hence, it follows that the electrode electric potential  $\varphi_{el}$  depends on the ion concentration in the solution in accordance with the logarithmic law:

$$\varphi_{el} = \varphi^{(0)} + \varphi_0 \ln c_i = \varphi_0 \ln \left( \frac{c_i}{c_i^*} \right), \quad (29)$$

where  $\varphi^{(0)} = (\mu^0 - \mu^m)/e$ ,  $\varphi_0 = k_B T/e$ , and  $\varphi^{(0)} = -\varphi_0 \ln c_i^*$ .

Equation (29) indicates that the electrode is not charged at the concentrations  $c_i = c_i^*$ , is positively charged for  $c_i > c_i^*$ , and is negatively charged for  $c_i < c_i^*$ . This equation holds true only for low-concentrated solutions. At high concentrations, it is necessary to use the so-called ion activity  $a_i$  instead of  $c_i$ . Formally, the activity is represented as  $a_i = f_i c_i$ , where  $f_i$  is the activity coefficient (a dimensionless quantity,  $f_i < 1$ ). This means that this activity is an effective ion concentration lower than the real concentration  $c_i$ . The fact is that the limiting stage in ion solutions is a drawing together of ions or their migration in external fields. Therefore, the introduction of the concept of activity permits taking into account the shielding effect of the ion cloud formed around an ion in high-concentrated solutions. It should be recognized, however, that such substitution is a formal expedient because the determination of ion activity is an extremely difficult task [2].

The second principal problem reduces to the prediction of the volt–ampere characteristic (VAC) of an electrode, which is frequently called the *polarogram* in electrochemistry [46–48]. This problem is usually addressed by elucidating the relationship between the total current  $j$  passing through the electrode and overvoltage  $\Delta\varphi$  found as the difference between an arbitrary value of the electrode potential  $\varphi$  and its equilibrium value  $\varphi_{el}$ . In this case, the electric circuit shown in Fig. 7 includes a voltage source. It should be emphasized that VACs in electrochemical systems may have different appearances and their shapes depend on a variety of factors. For this reason, it is necessary to specify in VAC classification the process that makes the main contribution to the formation of a current flow (this process is called the *limiting*

stage). Specifically, the limiting stage in an instant ion discharging is the ion transport toward an electrode. This process is described as *diffusion kinetics*. If the ion discharging takes finite time, it is interpreted in terms of the *slow discharge* theory [49]. Moreover, it should be borne in mind that electrochemical processes are essentially dependent not only on the ion type, composition of the solution, and material of the electrodes but also on the electrode surface structure (the presence of roughness, adsorption centers, oxide films, etc. [48]). These data indicate inevitably that electrode processes are especially intense at microtips of real electrodes, where the local electric field is many orders of magnitude stronger than the flat surface field. This fact constitutes the basis of such technologies as electrochemical polishing of metal surfaces, their passivation, and other procedures.

In the simplest case of discharging identical ions with a finite rate, the VAC was empirically determined by Tafel in 1905 as

$$\Delta\varphi = a + b \ln j,$$

where  $a$ ,  $b$  are certain constants.

Later on, this relationship was generalized and reduced to the form [46–49]

$$j = j_0 \left[ \exp \left( \frac{\alpha \Delta\varphi}{k_B T} \right) - \exp \left( - \frac{(1 - \alpha) \Delta\varphi}{k_B T} \right) \right], \quad (30)$$

where  $j_0$  is referred to as exchange current, and  $\alpha$  is the transport coefficient.

In multiion systems, the VAC usually has a stepwise form, with each step corresponding to an additional current induced by the onset of discharging of a specific ion type. An example is the VAC of an aqueous  $\text{PbCl}_2$  ( $10^{-3}$  mol) +  $\text{CdCl}_2$  ( $5 \times 10^{-4}$  mol) +  $\text{KCl}$  (1 mol) solution, shown in Fig. 9 (curve 1) [48]. Curve 2 corresponds to the VAC of a 1 mol  $\text{KCl}$  solution. It can be seen from the figure that curve 1 has two steps. One is due to the onset of discharging  $\text{Pb}^{2+}$  ions, and the other to the additional contribution from the discharging of  $\text{Cd}^{2+}$  ions. It needs to be noted that a microscopic theory explaining stepwise VACs of multiion systems remains to be developed. The importance of VACs was emphasized by the awarding of the Nobel Prize in Chemistry 1959 to the Czech scientist J Heyrovsky, their discoverer.

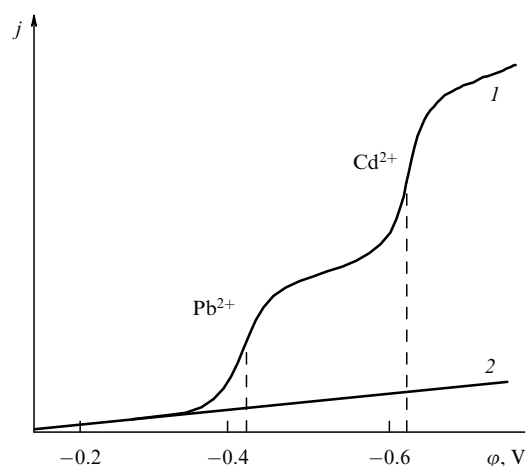


Figure 9. Polarograms (VACs) of a multiion system.

Practically all theoretical studies published over the last few decades have paid much attention to the derivation of formula (30) based on the liquid microstructure. The idea behind the theory is rather simple: it is necessary to take into consideration the solvent effect (ion *solvation* in electrochemical terms) and the influence of thermal fluctuations (in fact, phonons) on electron transitions. Some general results have been obtained in these studies, applicable to reactions in polar solvents; they are presented in a simplified form in monograph [49] and in more detail (based on quantum-mechanical calculations) in reviews [50, 51]. However, these results (as any first step) are insufficient because they disregard the real electrode surface structure and chemical properties of reactants. Despite the obvious fact that electron transition occurs during direct contact of an ion with the surface (which accounts for ion chemical sorption), it was stated [45, p. 93], in full conformity with theoretical considerations of electrochemists, that “The notion of ‘electron transitions’ in chemical sorption as transitions from the adsorbate to the adsorbent should be expelled from chemisorption and catalysis studies as the notion of electron orbits was expelled in its time from the atomic theory”. Such an opinion originates first and foremost from a different approach to the investigation of surface processes; it is based on the band model of conductivity that operates with such notions as *surface energy level* (instead of ion) and treats the problem of electron transfer from the electrode to the ion (or vice versa) as a transition from the bulk conduction band to the surface energy state [34, 44, 45]. We believe that the physically based approach is more sound because it allows us to more completely take into account peculiarities of the surface structure and electronic properties of both the electrode and the reactant. For example, in the case of transitions from the conduction band, it appears appropriate to use methods of physical kinetics, introducing such notions as mean free path, capture cross section, etc. On the other hand, quantum-mechanical (in fact, chemical) methods are more suitable for the analysis of transitions for localized states. Finally, electron transitions for surface states, where electrons can freely travel over the surface, or transitions within the gaseous phase should be expediently considered only in terms of physical kinetics [44].

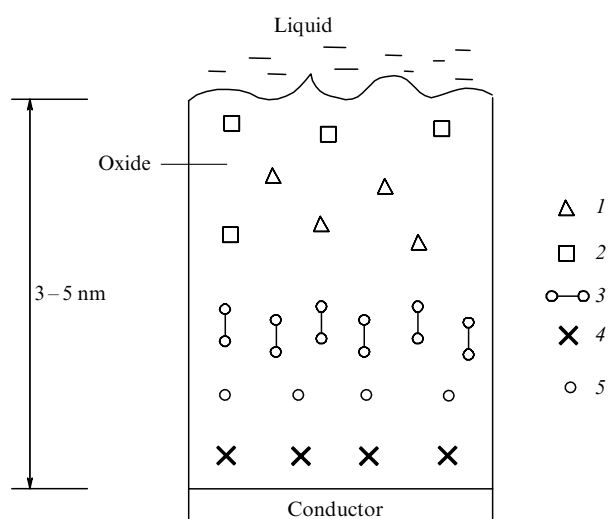
It is natural to pose a question: which of the well-developed and verified methods of computation of surface electron transitions can be used in application to the conductivity in high-voltage electric fields of both dense weakly conducting gases and liquid dielectrics? Obviously, the question is not easy to answer because a high-voltage field not only gives rise to new processes (e.g., cold electron emission, appearance of new surface electronic states as described in Section 5.2, etc.) but also causes restructuring of surface geometry (see review [27], where it was demonstrated convincingly). It was intimated in Section 5.1 that these processes take place in classical electrochemistry, too (e.g., electropolishing of the surface can be explained only by the fact that electrochemical reactions are especially intense at microtips of a rough electrode). It is no exaggeration to say that the classical concept of a flat surface with a DEL formed over it is restricted and actually of little value for the explanation of electron processes in high-voltage fields. We think that the classical approach applied with regard to geometric inhomogeneity of the surface may provide a deeper insight into the nature of surface electrophysical processes. This line of reasoning underlies the surface model

schematically presented in Fig. 3. One inference from the approach in question is that the charge distribution in the near-electrode region exposed to high-voltage electric field is qualitatively different from that described by classical electrochemistry and is quantitatively characterized by essentially different parameters.

The above considerations pose an important question of the physical sense of electron transition rate constants in reactions (4), (13) and their strength dependence for the external field responsible for these transitions. The answer to this question requires first elucidating the electronic structure of a solid surface in a high-voltage field and thereafter calculating the electron transition probabilities.

## 5.2 Surface electronic states

Surface electronic states (SESs) play an important role in the theory of semiconductors because they determine contact electronic properties [34]. The real surface of any metal is coated with an oxide film whose properties are closer to semiconducting ones; the same is true of any metallic electrode. By definition, SESs exist only in a narrow near-surface region where crystal properties are readily distinguishable from the properties of an infinite crystal lattice. This region is characterized by a nonuniform charge distribution both in parallel and perpendicular directions to the surface and it also contains specific electron adsorption centers associated with crystal lattice defects, geometric inhomogeneities, etc. By way of example, Fig. 10 [34] portrays the schematic distribution of surface electrons at



**Figure 10.** The structure of conductor–oxide heterojunction: 1 (2) — electron (hole) traps; 3 — slow, 4 — fast, and 5 — recombination electronic states.

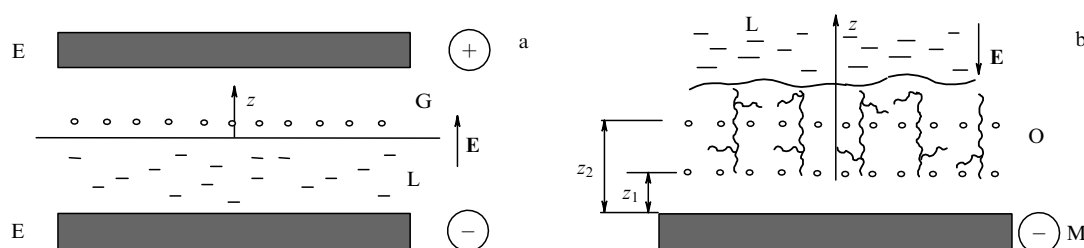
the edge of a silicon crystal coated with an  $\text{SiO}_2$  oxide film. It can be seen that SESs change in the direction from the free surface (i.e., silicon oxide) to the crystal as they pass from localized states 1, 2 (conditioned by the presence of traps originating from water molecule adsorption and the subsequent formation of  $\text{Si}-\text{OH}\dots\text{HO}-\text{Si}$  bonds) to slow 3 and fast 4 surface electron states, and finally to recombination states 5.

It should be emphasized that the oxidation of a metallic surface is a rather rapid process and the formation of oxide films is inevitable in experiments with typical metals (Al, Cu, and stainless steel). It was shown in Refs [61–63] that the exposure of initially nonoxidized electrodes of Al or stainless steel to the air for even 15 min results in appearing an oxide film on their surface that substantially reduces the breakdown voltage. According to the paper [64], the oxide film on the stainless steel surface consists of 90%  $\text{Cr}_2\text{O}_3$  and 10%  $\text{Fe}_2\text{O}_3$ . An air-oxidized copper electrode is coated with a 100–200-Å thick film of  $\text{Cu}_2\text{O}$  [65]. Moreover, the surface structure of an electrode (both its shape and composition) varies as current passes through it [13]. For example, copper iodide ( $\text{CuI}$ ) is formed at the surface of a nonoxidized copper electrode immersed in an iodine-containing transformer oil solution [66]; the copper iodide exhibits pronounced acceptor properties (approximately 4 times those of the nonoxidized Al surface [12]).

The passage of a current through thin dielectric films is accompanied by rather complicated processes (electron tunneling, luminescence, memory effects, etc.) depending on the film thickness, dielectric properties and structure of the film, external electric field strength, and so forth. This problem is being worked on fairly well due to its important implications for the development of semiconductor devices (see, for instance, a comprehensive review in the reference book [67]).

Assuming the oxide layer structure to be as presented in Fig. 10, the passage of a current can be described in terms of the following three processes: (1) electron transfer from the metal to the oxide layer; (2) capture of electrons in oxide layer traps and their transport to the oxide–liquid dielectric interface, and (3) activation charge transfer from the oxide layer to the liquid dielectric. Certainly, this scheme is amenable to modification, for example, in the case of a porous oxide layer (Fig. 11b) or in the region around a micropin tip where electrons can be captured directly by the traps (ions, electron acceptors) of a liquid dielectric. The volt–ampere characteristic is determined by the limiting stage; hence, each of the aforementioned processes needs to be considered separately.

In the case of so-called ohmic contact between the oxide and the metal in micron-thick films (in the absence of



**Figure 11.** The structure of electron layers: (a) over a liquid helium surface, and (b) in the porous oxide layer of a metal. Notations: E stands for electrode, G for gas, L for liquid, O for oxide, and M for metal.

tunneling) and free ion exchange between the oxide film and the dielectric, the limiting stage is the passage of current through the oxide in the so-called restricted space charge (RSC) regime. Simple calculations give the following dependence, first obtained by Mott and Gurney [67, 68]:

$$J = \frac{9\mu\epsilon\epsilon_0}{8d^3} U^2,$$

(31)

where  $d$  is the thickness of an oxide film,  $\epsilon$  is its permittivity,  $\mu$  is the charge (electron or ion) mobility in the film, and  $U$  is the voltage drop at the film borders (the potential difference between the metal and the oxide–dielectric interface).

Quadratic VACs are frequently observed in atmospheric corona discharges [69, 70] and in technical liquid dielectrics [9, 20, 31, 35, 37]. It is worth noting that VAC quadraticity is manifested regardless of the electrode shape (flat or pin-like), surface treatment technique, or special requirements for the properties of the liquid or the electrode material. This conclusion is exemplified by the results of studies [71, 72] where VACs in liquefied gases ( $H_2$ , He, Ar,  $O_2$ ) and benzene were measured in a tungsten pin–plane electrode system (with the radius of pin curvature  $\sim 10^{-4}$  cm, and the distance between the pin tip and the flat surface equal to 0.3 cm). Figure 12 shows a typical VAC, the initial segment of which is fairly accurately described by the quadratic dependence  $\sqrt{J} \sim 2.4U$ .

It is natural to consider the VAC of a gas corona discharge in connection with the contact ionization problem being discussed. Studies to this effect are well known, and we shall present only the results of our measurements for pin steel and copper electrodes in a pin–ring system (with a pin tip–ring distance of 6 mm, and radii of curvature  $\sim 0.04$  and  $\sim 0.05$  mm for Cu and Fe electrodes, respectively). The data obtained (Fig. 13) indicate that, for negative pins, the VAC does not depend on the electrode (curve 1 corresponds to Cu and Fe pins) material. On the contrary, VACs are substantially different in the case of positive pins (curve 2 corresponds to Fe electrodes, and curve 3 to Cu electrodes) when the ignition voltage is much higher. The initial segments of the VAC for negative pins are rather well approximated by the

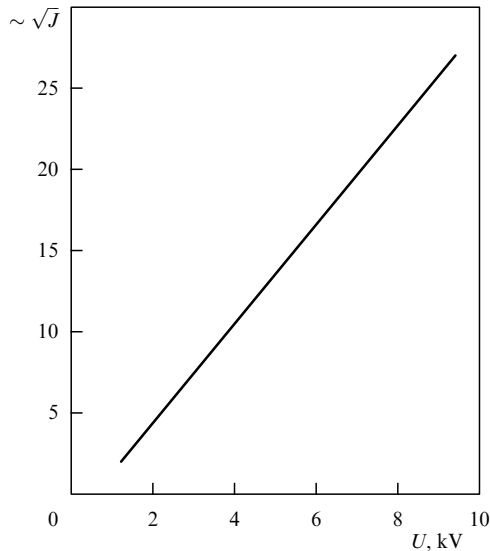
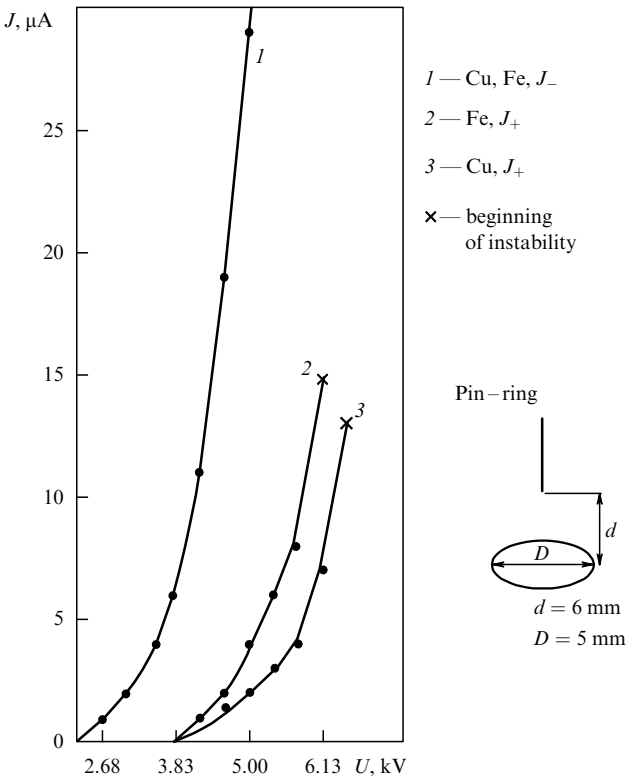


Figure 12. Volt–ampere characteristic in a pin (W)–plane electrode system in a liquid dielectric [71, 72].



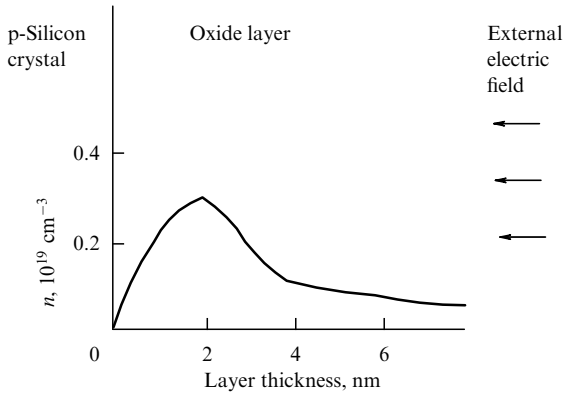
|    | $U/383, V$   | 7 | 8 | 9 | 10 | 11 | 12 | 13 | 14 | 15    | 16    | 17      |
|----|--------------|---|---|---|----|----|----|----|----|-------|-------|---------|
| Fe | $J_-, \mu A$ | 1 | 2 | 4 | 6  | 11 | 19 | 29 | 43 | 59–64 |       |         |
|    | $J_+, \mu A$ |   |   |   |    | 1  | 2  | 4  | 6  | 8     | 15–20 |         |
| Cu | $J_-, \mu A$ | 1 | 2 | 4 | 8  | 14 | 21 | 32 | 45 | 66    | 108   | 150–160 |
|    | $J_+, \mu A$ |   |   |   |    | 1  | 2  | 2  | 3  | 4     | 7     | 13–21   |

Figure 13. Volt–ampere characteristic of a corona discharge and the corresponding tabulated values.  $J_-(J_+)$  is the current for the negative (positive) pin.

quadratic expression  $J = 0.14u(u - 6)$ , where  $u = U/383$ , the voltage is measured in volts, and the current is measured in microamperes. This relation tends to be violated at voltages higher than  $U_* = 3.8$  kV. It is noteworthy that the critical value of  $U_*$  corresponds to the ignition voltage characteristic of a positive pin.

It is believed [21, 73–72] that only impact ionization occurs near the anode, whereas additional ionization takes place at the cathode where positive ions knock out electrons from the surface. Yet, there is thus far no definitive answer to the question of why the VAC for the positive pin so strongly depends on its material, while that for the negative pin is of a more universal character. Cold emission is unlikely to play here a leading role, bearing in mind that it is essentially dependent on the electron work function — that is, on the material of the electrode. We think that the most probable mechanism (consistent with the VAC quadraticity, low corona ignition voltage, and even the VAC’s universality) is the formation of weakly bound surface electronic states at the cathode at which electrons are readily knocked out by bare ions. This hypothesis is also strongly supported by the quadratic voltage dependence of the electron wind reaction force acting on the negative pin and rather accurately measured by Ostroumov [29].

While Eqn (31) accounts for VAC quadraticity, other regularities are in obvious conflict with it. Indeed, the



**Figure 14.** Electron bulk distribution in the inversion layer of p-silicon (quantum-mechanical computation [34]).

thickness of an oxide film changes with time even if it is exposed to the air, whereas the VAC remains unaltered. Complication of the RSC theory by the introduction of traps [67, 76] allows the temperature dependence of the VAC to be explained, but the relationship  $J \sim d^{-3}$  remains valid all the same. In our opinion, this approach to the explanation of a quadratic VAC in liquid dielectrics has no prospects; more sophisticated ideas taking into account the real surface structure are needed.

One way to address the problem is to postulate formation of a surface electron cloud in the oxide film coating a metal. Such states are known to exist in the inversion layer of p-semiconductors [34, 77–80] (Fig. 14) and in oxide films on metallic surfaces [81]. These states are quantized at low temperatures, while in the presence of an external magnetic field VACs exhibit some specific properties (Shubnikov–de Haas oscillations and quantum Hall effect [34, 77–80]).

The presence of a strong external electric field is responsible for ‘pulling out’ electrons into the outer region. This effect is well known and described in numerous publications (see, for instance, reviews [67, 82]). The most difficult task in the computation of surface electronic states of this type is to specify the one-electron interaction potential  $V_{\text{em}}$  with the conductor (a metal or semiconductor) and the dielectric. It is usually assumed that the main part of the potential, determined by image forces, is approximated by the expression

$$V_{\text{em}} = -\frac{\alpha}{z_* + z}, \quad (32)$$

where  $z_*$  is a constant; at the vapor–liquid helium interface  $\alpha = e^2(\varepsilon - 1)/[16\pi\varepsilon_0(\varepsilon + 1)]$ ,  $z_* = 1.05 \text{ \AA}$  [77, p. 24], and at the conductor–dielectric interface  $\alpha = e^2/(16\pi\varepsilon\varepsilon_0)$ .

Approximation (32) rather accurately describes the electronic state at the liquid helium surface due to the fact that the average distances  $z_i$  ( $i = 1, 2, \dots$ ) (see Fig. 14) at which surface electrons are essentially localized are greater than interatomic distances (for liquid helium,  $z_1 \approx 114 \text{ \AA}$ , and  $z_2 \approx 456 \text{ \AA}$ ) [77].

The absence of contact resistance indicates that the oxide layer at the metal surface is either metallized or irregular and porous. Therefore, we shall proceed from the conductor–dielectric surface model. Furthermore, the knowledge of the electron–conductor interaction needs to be supplemented by the calculation of the charge–dipole interaction potential  $V_{\text{ea}}$

between an electron and liquid molecules, i.e., charge solvation. In the continuous approximation, in the limit  $(a/z) \ll 1$  ( $a$  is the interatomic distance), one obtains

$$V_{\text{ea}} = \alpha \frac{\varepsilon - 1}{\varepsilon} \frac{1}{z}.$$

In this approximation, constant  $z_*$  in formula (32) can be omitted; then, the total potential is written down as

$$V = V_{\text{em}} + V_{\text{ea}} = -\frac{\alpha_1}{4z}, \quad \alpha_1 = \frac{e^2}{4\pi\varepsilon^2\varepsilon_0}. \quad (33)$$

Assuming the electron wave function being sought to have the form

$$\psi = \exp\left[-\frac{i}{\hbar}(E_s t - \mathbf{p}_1 \mathbf{r}_1)\right] f(z),$$

where  $\mathbf{p}_1, \mathbf{r}_1$  are the electron’s momentum and radius vector parallel to the surface, and  $E_s$  is the total electron energy, the equation for  $f(z)$  looks like

$$\frac{\hbar^2}{2m} f'' + \left(E - \frac{\alpha_1}{4z}\right) f(z) = 0, \quad E = E_s - \frac{p_1^2}{2m}.$$

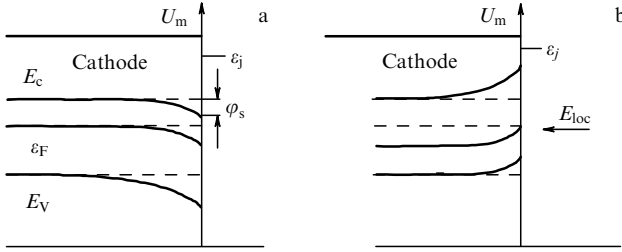
The solution of this equation is known from the hydrogen atom theory [86, 87]:

$$E = E_j = -\frac{I}{16\varepsilon^2 j^2}, \quad j = 1, 2, \dots, \quad (34)$$

$$f_j = A_j \xi \exp\left[-\frac{\xi}{2j}\right] P_{j-1}(\xi), \quad \xi = \frac{z}{z_0}, \quad (35)$$

where  $z_0 = 2e^2 a_0$ ,  $a_0 = 0.529 \text{ \AA}$  is the mean radius of a hydrogen atom,  $I = 13.55 \text{ eV}$  is its ionization potential, and  $P_{j-1}(z)$  is the polynomial of power  $j-1$ , such that  $P_{j-1}(0) = 1$ .

It follows from relationship (34) that wave functions at any  $j$  vanish at the surface ( $\xi = 0$ ) and exponentially decrease for  $z \rightarrow \infty$ ; in other words, they describe states localized over the conductor surface. The condition of their realization can be written in the form  $a/z_1 \ll 1$ , where  $z_1$  is the average distance between the surface and the first (ground) electronic state ( $j = 1$ ) described by the expression  $z_1 = 2z_0 = 4e^2 a_0 = 2.116e^2 \text{ \AA}$ . Because  $a \sim 1 \text{ \AA}$ , then  $a/z_1 \sim 0.5/\varepsilon^2$ ; hence, for typical  $\varepsilon \geq 2$ , the condition  $a/z_1 \ll 1$  is fulfilled in the first approximation. Thus, the surface electron layer in liquid dielectrics lies at a distance of several atomic radii or actually outside the conductor. When the electron concentration in this layer is sufficiently high, it may be expected that precisely these electrons determine electron exchange kinetics between the conductor and the traps in the dielectric. The assumption that the ground level energy equals  $E_1 \sim I/(16\varepsilon^2)$  leads to  $E_1 \sim 0.2 \text{ eV}$  for a nonpolar dielectric ( $\varepsilon = 2.1$ ), and  $E_1 \sim 0.8 \text{ eV}$  for gases. This means that these states are not destroyed by thermal fluctuations (at room temperature  $k_B T \sim 0.025 \text{ eV} \ll E_1$ ). The critical strength of an electric field influencing these states is estimated as  $E_* \sim E_1/(ez_1)$  and reaches several megavolts per cm by order of magnitude. Therefore, the effect of the external electric field on the energy of state in mean fields ( $\leq 100 \text{ kV cm}^{-1}$ ) can be neglected. Finally, in order to evaluate the contribution of localized surface electrons to surface processes, it is necessary to determine the population of these states.



**Figure 15.** The structure of energy bands in a semiconductor in the absence (a), and presence (b) of a high-voltage external field.

### 5.3 Population of surface states

Calculations will be made based on the conduction band theory taking the electron rest energy in the conductor as the zero level (Fig. 15). In this case, the energy of surface electrons is written as  $\varepsilon_j = U_m + E_j$  ( $E_j < 0$  and is found from Eqn (34), with  $U_m$  being the positive energy of electron–crystal lattice coupling). The number  $n_j$  of electrons in the conduction band with energy  $\varepsilon_j$  is linked to the electron concentration  $n_c$  in this band by the relationship  $n_j = n_c F(\varepsilon_j)$ , where  $F(\varepsilon)$  is the electron distribution function over energies. From the quantum standpoint, surface and energy electronic states in the conduction band with energy  $\varepsilon_j$  are indistinguishable, which implies a barrier-free exchange between them. This means that the wave function and its derivative for  $z \rightarrow 0$  must be continuous. Because the wave function vanishes at  $z = 0$ , the point  $z = 0$  in the conduction band is the node of the standing wave; in other words, the wave function in the vicinity of the surface has the form

$$\sqrt{n_j} \sin(k_j z) \exp \left[ -\frac{i}{\hbar} (\varepsilon_j t - \mathbf{p}_1 \mathbf{r}_1) \right].$$

By equalizing the derivatives of this function and expression (35) at  $z = 0$ , it is possible to derive the expression for the constant  $A_j$  in Eqn (35):  $A_j = z_0 k_j \sqrt{n_j}$ , where  $k_j = p_j / \hbar = \sqrt{2m\varepsilon_j} / \hbar$ . Hence, the surface concentration at the  $j$ -th level can be written down as

$$n_{sj} = n_j k_j^2 z_0^3 \beta_j, \quad \beta_j = \int_0^\infty f_j^2(\xi) d\xi.$$

The total surface concentration  $n_s = \sum_j n_{sj}$  is represented in the form

$$n_s = \lambda_s n_c \exp \left( -\frac{\chi}{k_B T} \right), \quad (36)$$

where  $\chi = U_m - \varepsilon_F$  is the work function in the case of metals ( $\varepsilon_F$  is the Fermi energy), and the parameter  $\lambda_s$  having dimension of length is expressed as

$$\lambda_s = z_0^3 \sum_j \frac{2m \varepsilon_j \beta_j}{\hbar^2} \exp \left( \frac{|E_j|}{k_B T} \right). \quad (37)$$

For the purpose of estimation, we shall restrict ourselves to the first member of sum (37) and then Eqn (36) can be written in the form

$$n_s = \lambda_1 n_c \exp \left( -\frac{E_A}{k_B T} \right),$$

$$\lambda_1 = \frac{z_0^3}{\hbar^2} 2m (\chi + \varepsilon_1) \beta_1, \quad E_A = \chi - |E_1|,$$

where  $E_A$  defines the activation energy of filling surface states from the conduction band.

It was estimated that  $\lambda_1 \sim 1 \text{ \AA}$ , and therefore the population of surface states is determined by the difference  $\chi - |E_1|$ . Because  $|E_1| \sim 1 \text{ eV}$ , the field strength peaks at low work functions ( $\chi \sim 1 \text{ eV}$ ), for example, when a metal is coated with a metallized oxide film that reduces them. In this situation, the maximum electron concentration  $n_{s^*}$  in surface layers may be rather high ( $n_{s^*} \sim 10^5 \text{ cm}^{-2}$  in semiconductors, and up to  $n_{s^*} \sim 10^{12} \text{ cm}^{-2}$  in metallized oxides).

### 5.4 Effect of an external electric field

In the presence of an external field, the electron concentration in the conduction band becomes a function of the electric field potential due to the so-called energy band bending effect [34, 44, 45]. By way of example, here is a case of intrinsic semiconductors [metals are considered in exactly the same way (see below)] when the  $z$ -component of the field strength and the electron concentration are expressed as

$$E_z = -E_* \sinh \frac{\varphi}{2\varphi_0}, \quad n_c = n_i \exp \left( \frac{e\varphi}{k_B T} \right),$$

$$E_* = \left( \frac{8en_i\varphi_0}{\varepsilon_n \varepsilon_0} \right)^{1/2}, \quad \varphi_0 = \frac{k_B T}{e},$$

$$n_i = n_0 \exp \left( -\frac{\Delta E}{k_B T} \right), \quad n_0 = \frac{(2\pi\sqrt{m_n m_p} k_B T)^{1/2}}{4\pi^3 \hbar^3},$$

where  $\Delta E$  is the forbidden band width,  $m_n(m_p)$  are effective electron (hole) masses, and  $\varepsilon_n$  is the dielectric constant of the semiconductor.

It should be recalled that  $\varphi$  is deemed to be zero inside the semiconductor (for  $z \rightarrow -\infty$ ). The use of electrodynamic conditions at the boundaries of the surface electron layer allows the following relationship that links the local field strength  $E_{loc}$  in a liquid (gas), the surface electron concentration  $n_s$ , and field  $E_z$  at the semiconductor surface to be derived:

$$\varepsilon_n \varepsilon_0 E_* \sinh \frac{\varphi_s}{2\varphi_0} - \varepsilon \varepsilon_0 E_{loc} = -en_s. \quad (38)$$

Consequently, in the absence of the external field,  $E_{loc} = 0$  and the surface potential  $\varphi_s < 0$ , in conformity with the energy bands bending downward (Fig. 15a). From the physical point of view, this means that the semiconductor surface is depleted of electrons and acquires a positive charge giving rise to a specific double layer. In the case of a negative electrode potential ( $E_{loc} > 0$ ), the potential  $\varphi_s$  becomes a function of the field strength  $E_{loc}$ . When  $n_s$  is written down in the form

$$n_s = n_{si} \exp \left( \frac{e\varphi_s}{k_B T} \right), \quad n_{si} = \lambda_s n_i \exp \left( -\frac{\chi}{k_B T} \right), \quad (39)$$

it is clear that at  $E_{loc} = E_i \equiv en_{si}/(\varepsilon \varepsilon_0)$  the potential  $\varphi_s = 0$ , while for  $E_{loc} > E_i$  the condition  $\varphi_s > 0$  will be fulfilled, which corresponds to the upward bending of the bands (Fig. 15b). By introducing variable  $x = \exp(e\varphi_s/k_B T)$ , relationship (38) can be represented as  $\mu x^2 + x - A = 0$ ,  $\mu = \varepsilon E_i/(\varepsilon_n E_*)$ , and  $A = \varepsilon E_{loc}/(\varepsilon_n E_*)$ . At typical values of  $n_i \sim 7.6 \times 10^{12} \text{ cm}^{-3}$  [83], one obtains  $E_* \sim 1 \text{ kV cm}^{-1}$ , while  $E_i < 1 \text{ V cm}^{-1}$ . For this reason, in strong electric fields

( $E_{\text{loc}} > 1 \text{ kV cm}^{-1}$ ), one finds  $\mu \ll 1$ , while  $A \gg 1$ . These inequalities indicate that the screening effect of surface electrons may be neglected. Thus, the potential  $\varphi_s$  in strong fields ( $A \gg 1$ ) is given by the expression

$$\sinh \frac{\varphi_s}{2\varphi_0} \sim \frac{1}{2} \exp \left( \frac{\varphi_s}{2\varphi_0} \right) = \left( \frac{\varepsilon}{\varepsilon_n E_*} \right) E_{\text{loc}}. \quad (40)$$

Taking into account the condition  $A \gg 1$ , formulas (38), (40) give the following dependence of surface electron concentration on the applied field strength:

$$n_s = n_{s0} \exp \left( \frac{\varphi_s}{\varphi_0} \right) = \eta_s E_{\text{loc}}^2, \quad (41)$$

$$n_{s0} = \lambda_s n_i \exp \left( -\frac{E_A}{k_B T} \right), \quad \eta_s = \frac{4n_{s0} e^2}{\varepsilon_n^2 E_*^2}.$$

It should be borne in mind that the external electric field has a rather strong influence on the population of surface levels; the concentration  $n_s$  in semiconductors may be as high as  $10^{10} \text{ cm}^{-2}$ , when the field strength amounts to hundreds of kilovolts per cm.

In the case of metals,  $E_* = (8en_0\varphi_0/\varepsilon_m\varepsilon_0)^{1/2}$ , where  $n_0$  is the free electron concentration in the bulk, and  $\varepsilon_m$  is the dielectric constant of the metal. In relationship (39),  $n_{si} = \lambda_s n_0 \exp(-\chi/k_B T)$ , and in formula (41)  $n_{s0} = \lambda_s n_0 \times \exp(-E_A/k_B T)$ , and  $\eta_s = 4n_{s0}e^2/\varepsilon_n^2 E_*^2$ .

### 5.5 Electron transition rate

Let us consider the reduction of  $A^+$  ions (or electron acceptor  $X$ ) at the cathode. The direct (from the electrode to the reducer) electrode current is defined as

$$i = \int_0^\infty P(z) n(z) dz, \quad (42)$$

where  $P(z)$  is the probability of transition of an electron to a single ion (atom) per unit time, and  $n(z)$  is the bulk concentration of the reducer. If the electron transfer occurs via direct contact of the electron with the electrode, formula (42) acquires the form

$$i = P(z_*) n(z_*) \delta z, \quad (43)$$

where  $z_*$  is the distance from the electrode at which the transfer takes place, and  $\delta z$  is the width of the transition region. According to Ref. [84], these parameters in gases are  $z_* \approx 4 \text{ \AA}$ ,  $\delta z \approx 0.2 \text{ \AA}$ . In liquids,  $n(z_*) \delta z$  needs to be perceived as the surface concentration of reducer ions (atoms). The probability  $P(z_*)$  is calculated by quantum mechanics and semiempirical methods reviewed in monograph [44]. The computation is based on the general idea that the total energy  $U$  of the complex ‘electrons (light system) — reducer atoms (heavy system)’ depends on its generalized coordinates  $q = (q_1, q_2, \dots, q_K)$  interpreted (e.g., in the case of polar solvents) as the angles of transverse phonon oscillations of dipoles and as the reactant coordinates of the electron system. The potential energies before ( $U_i$ ) and after ( $U_f$ ) the electron transition, as a function of the generalized coordinates, have the form of potential wells. The transition from the initial ( $U_i$ ) to the final ( $U_f$ ) state occurs through the activation mechanism due to the energy of thermal fluctuations. The equation  $U_i(q) = U_f(q)$  gives the values of coordinates  $q = q_*$  corresponding to the so-called transient

configuration of the system. In the case of classical motion of a system along all degrees of freedom (this condition is written out as  $\hbar\omega \ll k_B T$ , where  $\hbar\omega$  is the thermal phonon energy), the transition probability per unit time also has a classical form (see formula (4) in Ref. [50]):

$$w_{if} = \text{const} \times L_{if} \exp \left( -\frac{U_i(q_*)}{k_B T} \right), \quad (44)$$

where  $L_{if}$  is the electron exchange integral.

The application of formula (44) to concrete reactions is sometimes difficult, on the one hand because of excessive generalization, on the other hand due to the employment of a somewhat simplified model in which the atomic system is substituted by an abstract system of harmonic dipole oscillators. Such a situation is described in many theoretical works. As H Eyring ironically noted (see, e.g., Ref. [85]), “... the choice between mathematical and model approaches is reduced to the choice of time for the introduction of an approximation. In a model approach, approximations are introduced in the beginning, and in a formal one in the end”. This fact gives grounds for the development of simplified approaches that, on the one hand, provide a clear understanding of the physical mechanisms of electron transitions and, on the other hand, make it possible to derive formulas for estimates [34, 44, 45].

Formula (44) can be arrived at using a very simple method if the following simplifying assumptions are from the very beginning included in the formulation of the problem: (1) a single-electron problem is to be solved in which the electron transfers from a metal to an electronegative adsorbed atom (adatom); (2) electron–liquid interaction potentials in the continuous approximation depend only on the electron coordinate  $\mathbf{r}$ :  $U_{\text{ea}} = U_{\text{ea}}(\mathbf{r})$ , and electron–adatom  $X$  interaction potentials depend only on the atom ( $\mathbf{R}$ ) and electron coordinates:  $U_{\text{eX}} = U_{\text{eX}}(\mathbf{R}, \mathbf{r})$ , and (3) the transition occurs by virtue of electron–phonon interaction having the form  $U_{\text{e-ph}} = U_{\text{e-ph}}(\mathbf{r}) \exp(i\omega t)$ , where  $\omega$  is the phonon frequency.

In the framework of the adiabatic approximation [86, 87], the transition probability  $P$  per unit time is expressed as

$$P = \kappa \frac{1}{h} W_{if} \exp \left( -\frac{E_A}{k_B T} \right),$$

where  $h = 2\pi\hbar$ ,  $E_A$  is the transition heat equal to the difference between the final energy  $E_f$  of the electron–atom (including  $X$ ) system after the electron transition and the system’s energy  $E_i$  before the transition,  $E_A = E_f - E_i$ ;  $\kappa$  is the dimensionless function of temperature and  $E_A$ , and  $W_{if}$  is the square of the matrix element of the potential  $U_{\text{e-ph}}$ :

$$W_{if} = \left| \langle \psi_{\text{ea}}^i | U_{\text{e-ph}}(\mathbf{r}) | \psi_{\text{ea}}^f \rangle \right|^2,$$

where  $\psi_{\text{ea}}^i = \psi_{\text{ei}} \psi_{\text{ai}}$  ( $\psi_{\text{ea}}^f = \psi_{\text{ef}} \psi_{\text{af}}$ ) are the wave functions of the electron–adatom  $X$  system in the initial (final) state, described by the set of equations

$$\begin{aligned} \left[ -\frac{\hbar^2}{2m} \Delta_{\mathbf{r}} + U_{\text{eX}}(\mathbf{R}, \mathbf{r}) + U_{\text{ea}}(\mathbf{r}) + U_{\text{ext}}(\mathbf{r}) \right] \psi_{\text{e}} &= \varepsilon(\mathbf{R}) \psi_{\text{e}}, \\ \left[ -\frac{\hbar^2}{2m} \Delta_{\mathbf{R}} + U(\mathbf{R}) \right] \psi_{\text{a}} + L(\psi_{\text{a}}, \psi_{\text{e}}) &= E \psi_{\text{a}}, \end{aligned}$$

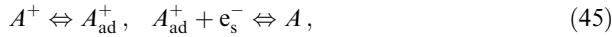
where  $U(\mathbf{R}) = E_{\text{a}}(\mathbf{R}) + \varepsilon(\mathbf{R})$  is the potential energy of the electron–adatom  $X$  system,  $E_{\text{a}}(\mathbf{R})$  is the energy of adatom  $X$

interaction with atoms (of a metal or a liquid),  $\varepsilon(\mathbf{R})$  is the electron interaction energy,  $U_{\text{ext}}(\mathbf{r})$  is the electron–external field interaction potential, and  $L(\psi_a, \psi_e)$  is the nonadiabaticity operator [86].

The expression for  $W_{\text{if}}$  acquires a transparent physical meaning if it is borne in mind that the electron–phonon interaction potential is proportional to the thermal fluctuation energy:  $U_{\text{e-ph}} \sim k_B T$ , yielding  $W_{\text{if}} \sim k_B T D_{\text{if}}$ , where  $D_{\text{if}} = |\langle \psi_{\text{ea}}^i | \psi_{\text{ea}}^f \rangle|^2$  is the square of the overlap integral proportional to the penetration coefficient through the potential barrier between two configuration states with energies  $U_i(\mathbf{R})$  and  $U_f(\mathbf{R})$ . This allows the electron transition probability to be written down in the classical form [5, 49]

$$P = \kappa \frac{k_B T}{h} D_{\text{if}} \exp\left(-\frac{E_A}{k_B T}\right).$$

In the absence of specific conditions (e.g., the presence of a high-voltage external field), it is usually assumed that electron transfers to adsorbed atoms are followed by product desorption into the gaseous or liquid phase [45]. For example, the process of  $A^+$  ion discharging can be written as



where  $A^+$  is the free ion,  $A_{\text{ad}}^+$  is the adsorbed ion, and  $e_s^-$  is the surface electron (either localized or present in the surface layer of the conduction band).

If  $n_{\text{si}}$ ,  $n_i$  denote respective concentrations of ions  $A_{\text{ad}}^+$ ,  $A^+$ , and  $n_e$  is the concentration of surface electrons, then reactions (45) are described by the equations

$$i = k_{\text{ad}} f_1 n_i - k_{\text{de}} n_{\text{si}}, \quad \frac{\partial n_{\text{si}}}{\partial t} = i - k_1 n_e n_{\text{si}}, \quad (46)$$

where  $i$  is the total  $A^+$ -ion flux density normal to the surface (including migration and diffusion currents),  $k_1$  is the electron transition rate constant,  $f_1 = 1 - n_{\text{si}}/n_{\text{so}}$  is the population coefficient of the surface reactive centers ( $n_{\text{so}}$  is the surface density of the reaction centers), and  $k_{\text{ad}}$  ( $k_{\text{de}}$ ) are adsorption (desorption) coefficients.

In the equilibrium conditions, Eqns (46) yield

$$i = k_1 n_e n_{\text{si}}. \quad (47)$$

Because adsorption–desorption processes are close to equilibrium, the first relationship in Eqn (46) indicates that the concentration  $n_{\text{si}}$  is determined by the Langmuir isotherm. Specifically, when the population coefficient  $f_1 \sim 1$  is small, we have  $n_{\text{si}} = K_s n_i$  ( $K_s = k_{\text{ad}}/k_{\text{de}}$ ), and formula (47) leads to Eqn (43). Constant  $k_1$  is defined as the product of the transition frequency  $\nu$  and electron capture cross section  $\sigma_e$ :  $k_1 = \nu \sigma_e$ . The flux density of discharging ions is described in terms of the physical parameters as

$$i = \nu \sigma_e K_s n_e n_i. \quad (48)$$

In estimations [44],  $\nu$  is perceived as the collision frequency of electrons from the conduction band with the reactant. Due to the high electron affinity of typical electron acceptors (e.g., the electron binding energy in an  $\text{I}_2^-$  ion equals 2.6 eV, in  $\text{Br}_2^-$  2.38 eV, in  $\text{O}_2^-$  0.43 eV, in  $\text{O}^-$  1.46 eV, and in  $\text{OH}^-$  1.83 eV [88, 89]), the capture cross section  $\sigma_e$  is usually described by the ion radius  $r_i$  ( $\sigma_e \sim \pi r_i^2$ ), and the coefficient  $K_s$  by the Langmuir isotherm. In fact, the product  $\nu \sigma_e n_e$  is the electron transition probability per unit time. In the case of an

adsorbed atom, it is determined by the time derivative of the electron transition probability  $w_{\text{if}}(t)$ , and in the case of an elastic collision by the product  $\nu w_{\text{if}}(\tau)$ , where  $\nu$  is the interatomic collision frequency ( $\nu = \bar{c}/(4l)$ ,  $\bar{c}$  is the atomic thermal velocity,  $l$  is the mean free path [90]) and  $\tau$  is the collision time. This means that in the case of elastic collisions the ion flux density is given by

$$i = \nu w_{\text{if}}(\tau) n_{\text{si}}. \quad (49)$$

The probability  $w_{\text{if}}(\tau)$  can be calculated by the methods of the quantum transition theory [86]. At any interaction potential  $W$ , the probability  $w_{\text{if}}(\tau)$  is proportional to the square of the matrix element  $\langle \psi_f | W | \psi_i \rangle$ , where  $\psi_i$  ( $\psi_f$ ) is the electron wave function in the initial (final) state. Because  $\psi_f = \psi_e \sim \sqrt{n_e}$ , it follows that  $w_{\text{if}}(\tau) = \sigma_e n_e$ . Elastic collisions with the surface involve only those ions that are located at a distance of a mean free path from it; hence,  $n_{\text{si}} = l n_i$ . Therefore, relationship (49) may be written in the form of formula (48) assuming that  $K_s = l$ :

$$i = \frac{1}{4} \bar{c} \sigma_e n_e n_i. \quad (50)$$

Here are some estimated parameters for electron transitions from surface layers. If it is assumed that  $\sigma_e = \pi d^2$ , the ion diameter  $d = 2$  Å, thermal velocity  $\bar{c} \approx 500$  m s<sup>−1</sup> (for oxygen  $\text{O}_2^-$  ion at room temperature  $\bar{c} \approx 440$  m s<sup>−1</sup>), typical ion concentrations in a weakly conducting gas  $n_i \leq 10^{18}$  cm<sup>−3</sup>, and surface density  $n_e = n_s = 10^4$  cm<sup>−2</sup>, then  $i \approx 10^5$  cm<sup>−2</sup> s<sup>−1</sup> (current density  $j = ei = 1.6 \times 10^{-14}$  A cm<sup>−2</sup>). This estimate indicates that discharging currents at an electrode having no potential are extremely low, but it undergoes electrization. In the presence of the potential, when the electric field at the electrode surface amounts to 10 kV cm<sup>−1</sup> or more, the discharging current is comparable to the experimentally found VAC ( $j \geq 10^{-10}$  A cm<sup>−2</sup>). It may be hypothesized that in sufficiently high electric fields in the initial part of the VAC in weakly conducting gases, the electron exchange (or electron knock-out) occurs largely with surface states. A weighty argument in support of this hypothesis is the initially quadratic VAC of a corona discharge (see Section 5.1 and also Refs [69, 70]). This inference ensues directly from Eqns (41), (50), while the threshold nature of the VAC can be related either to the onset of the fulfillment of the condition at which asymptotics (40) holds or to the achievement of the corona ignition voltage.

The initial nonlinearity of the VAC in liquid dielectrics almost invariably manifests itself in the form of quadratic dependence. This fact was for a long time interpreted in the framework of Ostroumov's hydrodynamic theory [29] according to which the limiting stage in the charge transfer is a convective (hydrodynamic) transport experimentally found to be quadratic with respect to the field strength. Later studies demonstrated that hydrodynamic flows are associated with injection conductivity at which the limiting stage is constituted by the charge generation process, while charge transfer plays a secondary role [35, 66]. The quadratic VAC in the conductivity injection regime is easy to explain on the assumption that electrons are captured by impurity electron acceptors from surface electron layers. For example, the rate constant  $k_1$  for reducing process (4) is expressed as

$$k_1 = \nu \sigma_e n_s.$$

Because  $n_s = \eta_s E_{\text{loc}}^2$  and in relatively weak fields  $\mu E_{\text{loc}} \gg k_{2X} G(E_{\text{loc}})$ , Eqn (5) gives the linear injection law [35, 66]

$$n_i = \eta_c E_{\text{loc}}, \quad \eta_c = \frac{v_{\sigma c} \eta_s}{\mu}.$$

It follows that the injection current is quadratic with respect to the field strength:  $j = e \mu n_i E = e \mu \eta_c \beta E^2$  ( $\beta$  is the field amplification coefficient).

## 6. Analysis of transient processes

This section deals with fast transient processes from which the main information about near-electrode processes is derived by the simplest methods — that is, using data on VAC and AT characteristics. There is a large variety of such experimental data, and it always appears possible to select relevant curves for verifying one theoretical postulate or another. Moreover, somewhat exotic works have been reported in which the authors tried to classify the VACs in liquid dielectrics based on their geometrical shapes [91]. In our opinion, such approaches are *a priori* doomed to failure because the formation of VAC and AT characteristics depends on many parameters and their combination may, generally speaking, produce such a great diversity of shapes that VAC classification will prove unproductive. It is necessary to distinguish limiting cases important either from the practical point of view or for the efficient measurements of electrophysical parameters of a weakly conducting medium. The most essential parameter is  $C = d/\xi_d$ , which may be used as a criterion. On the one hand, it determines the ratio of the nonequilibrium near-electrode layer thickness to the interelectrode gap size; on the other hand, it stands for the ratio of the field strength induced by impurity ions,  $E_i = e n_0 d / \varepsilon \varepsilon_0$ , to the external field strength:  $C = E_i / E_0$ .

Given that parameter  $C$  is small, charges in the interelectrode gap travel only under the effect of the external electric field; when the parameter  $C$  is large enough, the conductivity of the gap submits to the ohmic law. Therefore, further analysis will be governed by the value of  $C$ . It should be noted that the parameter  $C$  depends on the external field strength and may vary during measurements of the VAC (from large values in weak fields to small ones in strong fields). This explains why the theoretical computation of the VAC, in general, is a complicated problem resolvable only by numerical methods. It is much simpler as far as the assessment of AT characteristics is concerned due to the fact that  $C = \text{const}$  and there appears the possibility of separately studying the limiting cases of  $C \gg 1$  and  $C \ll 1$ .

It follows from physical considerations that the transition to a stationary state involves three fast processes, each having specific characteristic time, namely,  $t_D$  is the formation time of the near-electrode layers;  $t_r$  is the transition time of the dissociation–recombination reaction to equilibrium, and  $t_e$  is the time of ion wave propagation. Each process will be individually analyzed in Sections 6.1–6.3 below in order to determine the afore-mentioned characteristic times and the related parameters. The processes will be considered in the following order. First, the weak field region is discussed, where  $C \gg 1$  and the transient process is characterized by the time  $t_r$  of transition of the dissociation–recombination reaction to equilibrium. Thereafter, transient processes triggered by a sudden switching on of the constant external electric field for  $C \ll 1$  are analyzed.

### 6.1 Transition of dissociation–recombination reactions to equilibrium

The transient process for  $C \gg 1$  is associated with the transition of reaction (2) to equilibrium. Under uniform external conditions, the concentrations of  $A^+$ ,  $B^-$  ions are identical,  $n_1 = n_2 = n(t)$ , and depend only on time; therefore, the transient process is described by an equation ensuing from Eqn (8):

$$\frac{dn(t)}{dt} = k_d N - \alpha_{11} n^2(t), \quad t = 0 : n = 0. \quad (51)$$

In this equation, the ion pair concentration  $N$  is assumed to be constant because the degree of ion dissociation is insignificant ( $n/N \approx 10^{-5}$  [8]). Evidently, as  $t \rightarrow \infty$ , the limit  $n(t) \rightarrow n_0 = \sqrt{k_d N / \alpha_{11}}$  holds.

The solution of problem (51) has the form

$$n(t) = n_0 \frac{1 - \exp(-t/t_r)}{1 + \exp(-t/t_r)}, \quad t_r = \frac{1}{2\alpha_{11}n_0}. \quad (52)$$

It can be seen that the parameter  $t_r$  determines the time of transition of reaction (2) to equilibrium. By expressing  $\alpha_{11}$  through the mobility (the Langevin formula [8]), one arrives at  $t_r = \tau_c/2$ , where  $\tau_c = \varepsilon \varepsilon_0 / \sigma$  is the relaxation time of free charges in a medium with ohmic conductivity. For technical dielectrics with a typical conductivity  $\sigma = 10^{-10} \text{ } \Omega\text{m}^{-1}$  and nonpolar dielectrics ( $\varepsilon = 2$ ), one finds  $t_r = 0.1 \text{ s}$ ; in other words, the process in question is rather fast, comparing  $t_r$  with the characteristic observation time ( $\sim 1 \text{ s}$ ), and slow if  $t_r$  is compared with the time of ion wave propagation.

### 6.2 Time of ion wave travel

Ion waves in a liquid dielectric can be observed only under specific conditions, for example, in well-purified fluids. Mathematically, these conditions can be specified by one inequality

$$C = \frac{d}{\xi_d} \ll 1. \quad (53)$$

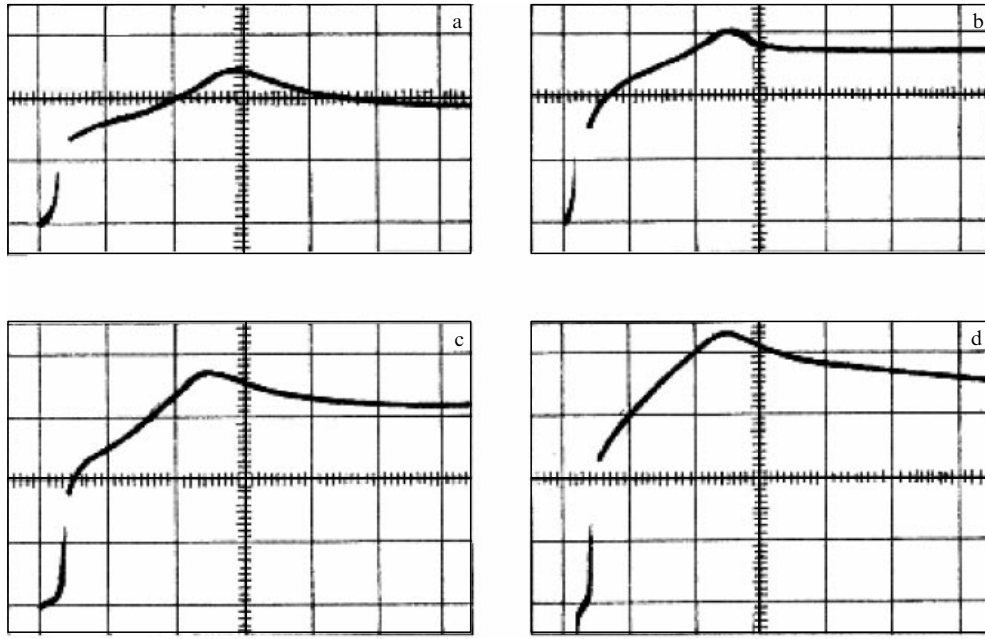
The physical sense of inequality (53) is obvious, namely, the nonequilibrium region extends over the entire interelectrode gap, the intensity of the recombinative interaction between charges is very low, and, finally, the field induced by a bulk charge is significantly weaker than the external field. In this case, the electric field is an external one, and the equations of charge motion (8) become homogeneous hyperbolic equations.

Characteristic times of positive ( $t_{e1}$ ) and negative ( $t_{e2}$ ) wave propagation are described [6] as

$$t_{ej} = \frac{d}{\mu_j E_0}, \quad j = 1, 2, \quad (54)$$

where  $E_0 = U/d$  is the constant external electric field.

Formula (54) forms the basis for evaluating the mobility of ions by the time-of-flight method [9, 10]. With this technique, ions are usually injected into a liquid or produced by a radioactive source. Of primary interest, however, is the measurement of the mobility of impurity ions themselves, the type of which is frequently unknown and, generally speaking, needs to be determined. The measurement of mobility exactly yields the necessary information. For example, it has been demonstrated in Ref [8] based on the assessment of the VAC that the effective radius of negative ions in an iodine-



**Figure 16.** Ampere–time characteristics in benzene [92]: (a)  $E = 5.6 \text{ kV cm}^{-1}$ , (b)  $E = 6.4 \text{ kV cm}^{-1}$ , (c)  $E = 7.2 \text{ kV cm}^{-1}$ , and (d)  $E = 8 \text{ kV cm}^{-1}$ . Across —  $5 \times 10^{-2} \text{ s}$  per scale division; down —  $10^{-8} \text{ A}$  per scale division.

containing transformer oil solution is on the order of  $12 \text{ \AA}$ ; this means that these ions are complex structures.

The mobility of impurity ions is evaluated from AT characteristics [92–94] whose typical shape is depicted in Fig. 16. It is generally accepted that the distance from the origin of the curve to its first maximum along the time axis determines the time of ion flight [92–94]. Unfortunately, the criterion (53) was not verified in the majority of published works and, in my opinion, time-of-flight estimates were incorrect. As a result, the authors of these studies failed to provide information (about electrode area, initial ohmic conductivity, etc.) sufficient for the required processing of experimental data. It is therefore appropriate to make estimates based on the typical characteristics of well-purified benzene [92], including  $d = 2.5 \text{ mm}$ ,  $\varepsilon = 2$ ,  $\sigma = 10^{-14} \Omega^{-1} \text{ cm}^{-1}$ ,  $E_0 = 4 \text{ kV cm}^{-1}$ , and  $\mu_1 \sim \mu_2 = 5 \times 10^{-4} \text{ cm}^2 (\text{V s})^{-1}$ . Criterion (53) can be written in the form

$$C = \frac{\sigma d}{(\mu_1 + \mu_2) \varepsilon \varepsilon_0 E_0},$$

which gives  $C = 3 \times 10^{-3}$ ; in other words, condition (53) is fulfilled.

The experimentally obtained AT curves [93] show small peaks (see Fig. 16), whereas physical considerations suggest that the current must monotonically decrease following a broken line (see text below). We believe that the ascending section of the AT curves reflects a transient process in the measuring device (that always has its own capacity), while the dropping sections describe the final stages of ion wave propagation.

These data emphasize the necessity of analytical computation of AT characteristics: first, for the elucidation of physical mechanisms underlying transient processes, and, second, for the time-of-flight determinations from the AT curve.

The presence of the small parameter  $C$  on the right-hand sides of nonstationary Eqns (7), (8), after they are brought to

a dimensionless shape, makes it possible to solve the problem by methods of the perturbation theory, namely, by representing the field  $E_x$  and charge density  $n_j$  ( $j = 1, 2$ ) in the form [to recall, the consideration applies only to a flat capacitor (see Section 3)]

$$E_x = E_0 + E_1 + \dots, \quad n_j = n_{j0} + n_{j1} + \dots, \quad (55)$$

where terms  $E_1$ ,  $n_{j1}$  are linear with respect to the small parameter  $C$ , and  $E_0 = U/d$  is the constant external field.

Only the final result of cumbersome calculations is presented here, omitting details. To begin with, Eqns (7), (8) in the case of a flat capacitor and a two-ion model ( $n_4 = 0$ ) have the integral

$$j_0(t) = \varepsilon \varepsilon_0 \frac{\partial E_x}{\partial t} + e(\mu_1 n_1 + \mu_2 n_2) E_x, \quad (56)$$

where  $j_0(t)$  should be interpreted as a current in the external circuit, the first term on the right-hand side is the displacement current, and the last term is the migration current.

After the definition of expansions (55) and their substitution into Eqn (56) we get, up to the linear terms, the following results:

$$j(t) = j_e(t) + j_i(t) + j_d(t), \quad (57)$$

$$j_e(t) = \varepsilon \varepsilon_0 \left. \frac{\partial E_1}{\partial t} \right|_{x=0},$$

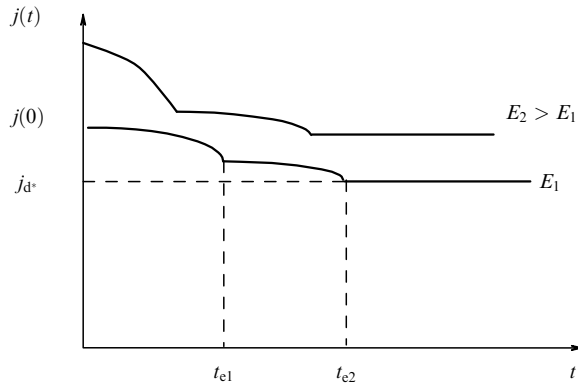
$$j_i(t) = e(\mu_1 n_{10} + \mu_2 n_{20}) E_0 + e\mu_2 n_{20} E_1|_{x=0},$$

$$j_d(t) = e\mu_2 n_{21}|_{x=0} E_0,$$

$$E_1|_{x=0} = \frac{en_0}{\varepsilon \varepsilon_0 d} \left[ (x_1 + x_2) d - \frac{d^2}{2} - \frac{1}{2} (x_1^2 + x_2^2) \right],$$

$$n_{21}|_{x=0} = \left( k_d N - \mu_2 \frac{en_0^2}{\varepsilon_0 \varepsilon} \right) \frac{x_1}{V_2}, \quad t \leq t_*;$$

$$n_{21}|_{x=0} = k_d N \frac{d}{V_2} - \mu_2 \frac{en_0^2}{\varepsilon \varepsilon_0} \frac{x_2}{V_2}, \quad t > t_*.$$



**Figure 17.** The overall view of AT characteristics in the case of  $C \ll 1$  and for  $\mu_1 > \mu_2$ .

Here,  $x_1 = V_1 t$ ,  $x_2 = d - V_2 t$ , and  $V_j = \mu_j E_0$  are the equations for wave front motions of positive ( $j = 1$ ) and negative charges;  $t_* = d/(V_1 + V_2)$  is the time of their meeting ( $x_1(t_*) = x_2(t_*)$ );  $j_e(t)$  is the displacement current;  $j_0(t)$ ,  $j_{11}(t)$  are ion wave currents in the zero and first approximations;  $j_d(t)$  is the dissociation current, and  $E_0 = U/d$  is the external electric field.

Functions  $n_{10}$ ,  $n_{20}$  are also time-dependent and defined as

$$n_{10} = \begin{cases} 0, & 0 \leq x \leq x_1, \\ n_0, & x_1 < x \leq d, \end{cases} \quad n_{20} = \begin{cases} n_0, & 0 \leq x \leq x_2, \\ 0, & x_2 < x \leq d. \end{cases}$$

In relationships (57),  $x_j$  should be regarded as linear functions till the relative instants of time  $t_{ej} = d/V_j$ :  $x_1 = d$  for  $t > t_{e1}$ , and  $x_2 = 0$  for  $t > t_{e2}$ .

Examination of expression (57) indicates that the AT characteristic has the form of a monotonically descending broken curve with the maximum at the origin (Fig. 17). The slope of the curves changes at two points  $t = t_{e1}$ ,  $t = t_{e2}$  corresponding to two pulsed ion waves. The initial current is always the highest and defined as  $j(0) = \sigma E_0$ ,  $\sigma = e(\mu_1 + \mu_2)n_0$ , while saturation depends on the dissociation current: for  $t \geq \max(t_{e1}, t_{e2})$ , it is  $j = j_d = ek_d Nd$ . The ratio  $j_d^*/j(0) \approx C \ll 1$ , i.e., the smaller the parameter  $C$ , the larger the jump. This explains why AT characteristics for  $C \geq 1$  have the form of straight lines. Because the dissociation rate constant is a function of the field strength,  $k_d = k_{d0}F(E)$  (where  $F(E)$  is the Onsager factor [1, 8]), the AT curve ascends as the field grows, and the kink points shift to the left (see Fig. 17). Comparison of these inferences with the data in Fig. 16 shows that the positions of current maxima (in time) are only weakly dependent on the field strength. This confirms the opinion that the growth of current at the initial sections of AT curves should be attributed to transient processes in the measuring device. The above inferences are in good agreement with those sections of AT curves that describe a decrease in current with time.

### 6.3 Near-electrode transient processes

When criterion (53) is fulfilled, AT characteristics contain information not only about times of flight found from the kink points but also about charge accumulation in the diffusion layer at finite ion discharging times. As noted in Section 4, accumulation of charges in the diffusion layer leads to the formation of a surface charge  $q_s$ . By measuring this charge and using Eqn (27), it is possible to calculate the

coefficient of field amplification by the diffusion layer and estimate electron transition rate constants.

This inference is substantiated by the following line of reasoning, also applicable to the case of  $C \gg 1$ . Under stationary conditions outside the diffusion layer, the transient time of its formation is estimated from the relationship  $t_D \approx \xi_D/(\mu_1 E_V)$ ; it is very small because the size of the diffusion layer is small, too. The process of charge accumulation is then described by Eqns (12), and it is convenient to bring them to the integral form by integrating the charge balance equations in a range from  $x = r_0$  to  $x = \xi_D$ :

$$j^+ = j_{1x}|_{x=r_0} = \frac{\partial q_{1s}}{\partial t} + j_{1v}, \quad q_{1s} = e \int_{r_0}^{\xi_D} n_1 dx.$$

The former relationship is analogous to expression (56) and indicates that the contribution of positive charge current  $j^+$  to the current in the external circuit consists of the displacement current  $\partial q_{1s}/\partial t$  due to the charge accumulation in the diffusion layer and the migration current  $j_{1v}$  expressed as  $j_{1v} = e\mu_1 n_{1v} E_V$  in the case of  $C \gg 1$ , and as the dissociation current  $j_{1v} = ek_d Nd$  (after the passage of ion waves) in the case of  $C \ll 1$ . Current  $j^+$  being an experimentally determined variable, and  $j_{1v}$  calculable theoretically, the difference between them determines the charge accumulation rate  $\partial q_{1s}/\partial t$  in the diffusion layer. After the transient process in the external circuit terminates, it is possible to calculate the steady-state value of  $q_{1s}$  and thereafter find the coefficient of field amplification  $\beta_D$  by the diffusion layer using Eqn (27).

## 7. Conclusions

The studies reviewed in this paper brought about the following results.

(1) The near-electrode region is shown to consist of a  $\xi_d$ -thick layer where nonequilibrium dissociation–recombination reactions occur and a  $\xi_D$ -thick diffusion layer subdivided into two sublayers: an adsorptive one, and a diffusion sublayer proper.

(2) The coefficient  $\beta_D$  of local field amplification by the diffusion layer was calculated. The total amplification coefficient to which both the diffusion layer and the geometry of micropins contribute is a product of the respective coefficients:  $\beta = \beta_D \beta_s$ , so that  $E_{loc} = \beta E_s$ , where  $E_s$  is the mean field at a smooth surface.

(3) Comparative analysis of experimental methods and theoretical approaches to study electron transfer kinetics in electrolytes and weakly conducting media (liquid dielectrics and dense gases) demonstrated the importance of taking into consideration the real structure of electrode surfaces and the contribution of surface electrons to contact charge generation not only in liquid dielectrics but also in electrolytes and gases.

(4) The analysis of electronic states in surface layers and the kinetics of electron transfers from an electrode to an electron acceptor in both liquid and gaseous phases gave evidence that quadraticity of the initial VAC portions in sufficiently strong electric fields may be due to electron transitions (or electron knock-out in the gaseous phase) from the surface states.

(5) The analysis of transient processes and forms of AT characteristics showed that ion waves are generated only when the criterion  $d/\xi_d \ll 1$  is fulfilled, while the kink points of AT curves may be used for evaluating the ion mobility.

(6) Experimental AT characteristics are consistent with theoretical predictions only at the descending sections of the curves. The source of the maxima in the experimental AT curves remains to be elucidated.

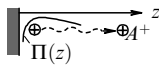
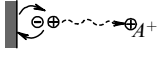
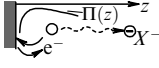
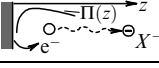
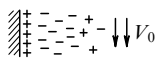

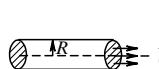
(7) AT characteristics may be used to determine the amplification coefficient  $\beta_D$ ; the resulting value taken together with the measured data for the capacitance of the diffusion layer makes it possible to calculate the rate constants of the ion discharging reaction at the electrodes.

In light of the above findings, it is natural to consider the role of surface electronic states and real properties of the surface in contact electrophysical and electrochemical processes proceeding both in electrolytes and weakly conducting media.

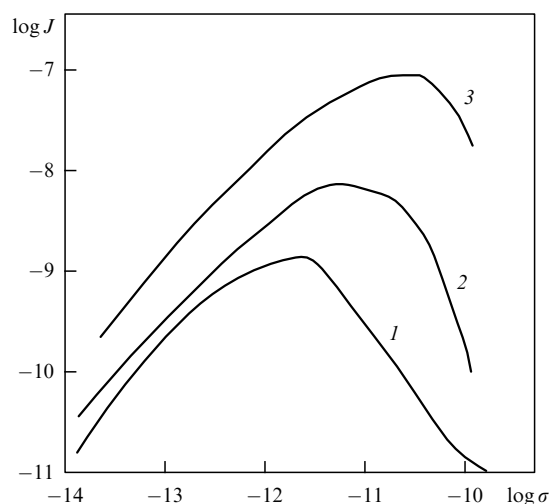
**Electrolytes.** The concept of the DEL on a flat electrode surface is clearly obsolete. It disregards amplification of the external field at micropins, known to markedly intensify the electrochemical process. This phenomenon is of special importance in reactions where electrodes undergo dissolution or the reaction products are released at their surfaces. In our opinion, novel approaches are first and foremost needed to prolong the service life of electrochemical devices. One such approach is to introduce effective density  $\eta_s$  of micropins at which electrochemical reactions proceed with the largest rates. Another problem of primary importance that awaits resolution concerns electrochemical processes at micropins taking into consideration field amplification due to the geometric factor and the structure of electronic states near the surface. The solution of this problem would bring an expression for the total current  $i_s$  at a micropin as a function of the mean field  $E$ . In this case, the resulting average current density  $i$  is given by the product  $i = \eta_s i_s$ . Such an approach remains to be developed in further studies.

**Liquid dielectrics.** It appears from published reviews [1 – 13] that there is a sort of unwritten agreement on how to understand and interpret some general processes in the bulk of liquid dielectrics, at least at small concentrations of ion components and in the weak field region. The problem of contact electrophysical (and sometimes electrochemical) processes has not thus far been properly touched upon in the scientific literature. The treatment of liquid dielectrics as insulators leads to the conclusion that contact processes in the weak field region are insignificant, being characterized by extremely low currents, small concentrations of impurity ion components, etc. The difficulty in studying them and low demand for the practical use of these materials may account for the current situation. However, the recently emerged areas of technical application of electrohydrodynamic flows, first of all to heat exchange intensification [95, 96], has aroused a new wave of interest in the problem of electroconductivity of liquid dielectrics. This again necessitated elucidation of ionization mechanisms. The predominant model for the purpose has for a long time been the ohmic conductivity law  $\mathbf{j} = \sigma \mathbf{E}$ , where the coefficient of conductivity was a function of temperature and the electric field strength module,  $\sigma = \sigma(T, E)$  [11, 29, 97, 98]. From the physical point of view, this means that conductivity is realized in the conditions of the equilibrium ion pair dissociation – monoion recombination reactions. However, this approximation holds only for relatively weak fields where the condition  $d/\xi_d \gg 1$  is satisfied. This condition is violated in strong enough fields (e.g., near pin electrodes); therefore, both the conductivity and the concomitant electroconvection have to be investigated using a multiion conductivity model with charge injection from the electrodes [16, 17, 33, 66]. It is this circumstance that has given new impetus to a greater interest

**Table 1.** Physical – chemical schemes and formulas for the calculation of injection processes of electrolyzation in liquid dielectrics.

| Process  | Injected charge density  | Injected current density   | References | Physical – chemical scheme  |
|--|--|--|------------|---|
| Shottky injection  | $q_\infty = q_A \frac{\exp(-\xi_{ad}/r_A)}{bK_1(b)}$   | $J_i = \mu q_\infty E$   | [36]       |  |
| $M + A^+ B^- \rightleftharpoons M(e) + A^+ B \rightarrow A_{free}^+$ | $q_\infty = \frac{J_i}{\mu_+ E}$   | $J_i = \frac{e\alpha_{ext} \alpha_{ox} N}{\alpha_{rd} + \alpha_{ext}}$ | [19]       |  |
| $X + e^-(M) \rightleftharpoons X^-$                                  | $q_i = \frac{ek_1 X c_X}{\mu E_{loc} + k_2 X G(E_{loc})}$  | $J_i = \mu q_i E$  | [35]       |  |
| $X + e^-(M) \Rightarrow X^-$   | $q_i = \eta_i E$   | $J_i = \mu \eta_i E^2$   | [35]       |  |
| Adsorptive electrization   | Electrization current<br>$J = (q_{s2} - q_{s1}) S V_0, \quad S = 2\pi r_D R,$<br>$q_{sj} = K_{ad,j} q_0, \quad j = 1, 2$<br>$J = \sqrt{2e\epsilon n_* \varphi_0} 2\pi R V_0,$<br>$n_* = n_A / K_{ad}, \quad n_A = (k_1/k_2) c_A, \quad \varphi_0 = k_B T/e,$<br>$K_{ad} = \int_{x_A}^{\infty} \exp(\xi_{ad}/x) dx$ |  |            |  |
| Electrization by the redox mechanism                                 |  |  |            |  |
| $A + e^-(M) \rightleftharpoons A^+$                                  |  |  |            |  |

**Notations:**  $\xi_{ad}$  — radius of action of short-range forces found from Eqn (21);  $r_A$  — ion radius;  $b = 2(eE_{loc}/16\pi\epsilon\epsilon_0)^{1/2}/\varphi_0$ ;  $K_1(b)$  — modified first-order Bessel function;  $\Pi(z) = -e^2/(16\pi\epsilon\epsilon_0 z) - eEz$ ;  $\alpha_{ox}(\alpha_{rd})$  — rate constant of the direct electron transfer from an ion to the electrode (reverse transfer from the electrode to a reaction product), and  $\alpha_{ext}$  — rate constant of injection from the electrode surface into the liquid.



**Figure 18.** The dependence of electrization current on n-heptane conductivity at different flow velocities  $v_0$  in a cylindrical platinum tube with a radius of 0.07 cm [55]: 1 —  $v_0 = 1.5 \text{ m s}^{-1}$ ; 2 —  $v_0 = 3.35 \text{ m s}^{-1}$ , and 3 —  $v_0 = 10.9 \text{ m s}^{-1}$ .

in contact processes in the weak and mean field regions (up to  $20\text{--}40 \text{ kV cm}^{-1}$ ).

In addition to the problem of studying liquid dielectrics in an electric field, there is a long-standing and poorly known problem of static electrization of weakly conducting media. This problem from time to time attracts the attention of researchers [55–59] but its solution is still far from being found. We have already mentioned two approaches to static electrization: one based on the adsorptive mechanism with the formation of a DEL (when the contact medium is a dielectric), and the other on the redox mechanism (in metals). Table 1 presents a summary of results on injection currents in an electric field and electrization currents obtained in the framework of the simple models. Doubtlessly, these results do not reflect the overall picture of complex contact processes and are of value solely for the purpose of estimation. Suffice it to point out the experimentally found extreme dependence of the electrization current on the ohmic conductivity coefficient of a hydrocarbon liquid in order to illustrate the unusual and enigmatic nature of the problem in question (see Ref. [55] and Fig. 18). We believe that the problem of static electrization must also be resolved in the framework of the multiion model [35] taking into consideration dissociation–injection processes in bulky liquids and contact processes at the surface with due regard for its real structure.

**Weakly ionized dense gases.** The role of contact processes involving electrons in surface states may be very important at the initial stage of corona discharge, for example, when ‘primer’ charges are formed that induce avalanche-like impact ionization of neutral atoms (molecules) in the bulk. Moreover, surface electronic states being the least energetically bound ones may cause electrization of bodies in a gaseous medium containing electronegative molecules. It is certainly a low-current region, but charge accumulation during a long period (or under intense flow around the body) may be very significant and these processes cannot be disregarded. We think that the process of ionization of dense gases, for example, the air, by the redox mechanism requires further experimental and theoretical studies.

## References

1. Onsager L J. *Chem. Phys.* **2** 599 (1934)
2. Izmailov N A. *Elektrokhimiya Rastvorov* (Electrochemistry of Solutions) (Moscow: Khimiya, 1966)
3. Gordon J E. *The Organic Chemistry of Electrolyte Solutions* (New York: Wiley, 1975) [Translated into Russian (Moscow: Mir, 1979)]
4. Tomilov A P et al. *Elektrokhimiya Organicheskikh Soedinenii* (Electrochemistry of Organic Compounds) (Leningrad: Khimiya, 1968) [Translated into English (New York: Halsted Press, 1972)]
5. Caldin E. *Fast Reactions in Solution* (New York: Wiley, 1964) [Translated into Russian (Moscow: Mir, 1966)]
6. Szwarc M. *Carbanions, Living Polymers, and Electron Transfer Processes* (New York: Interscience Publ., 1968) [Translated into Russian (Moscow: Mir, 1971)]
7. Szwarc M (Ed.) *Ions and Ion Pairs in Organic Reactions* (New York: Wiley-Interscience, 1972–1974) [Translated into Russian (Moscow: Mir, 1975)]
8. Zhakin A I. *Usp. Fiz. Nauk* **173** 51 (2003) [*Phys. Usp.* **46** 45 (2003)]
9. Gallagher T J. *Simple Dielectric Liquids: Mobility, Conduction, and Breakdown* (Oxford: Clarendon Press, 1975)
10. Adamczewski I. *Jonizacja i Przewodnictwo Cieklych Dielektryków* (Warszawa: Naukowe, 1965) [Translated into English: *Ionization, Conductivity and Breakdown in Dielectric Liquids* (London: Taylor & Francis, 1969); translated into Russian (Leningrad: Energiya, 1972)]
11. Skanavi G I. *Fizika Dielektrikov: Oblast' Slabykh Polei* (Physics of Dielectrics: Weak Field Region) (Moscow-Leningrad: Gostekhzdat, 1949)
12. Kargin V A (Ed.) *Organicheskie Poluprovodniki* (Organic Semiconductors) (Moscow: Nauka, 1968)
13. Lewis T, in *Progress in Dielectrics* Vol. 1 (Eds J B Birks, J H Schulman) (New York: Wiley, 1959) [Translated into Russian (Moscow-Leningrad: Gosenergoizdat, 1962) p. 7]
14. Moreau O et al., in *Proc. of 1996 IEEE 12th Intern. Conf. on Conduction and Breakdown in Dielectric Liquids, Rome, Italy, July 15–19, 1996* (New York: IEEE, 1996) p. 405
15. Zhdanov S I, Gracheva I P, in *Zhidkie Kristally* (Liquid Crystals) (Ed. S I Zhdanov) (Moscow: Khimiya, 1979) p. 35
16. Felici N J. *Direct Current* **2** 90 (1971)
17. Felici N J. *Direct Current* **2** 147 (1971)
18. Voinov M, Dunnett J S J. *Electrochem. Soc.* **120** 922 (1973)
19. Castellanos F, in *Electrohydrodynamics* (CISM Courses and Lectures, No. 380, Ed. A Castellanos) (Wien: Springer, 1998) p. 1
20. Zhakin A I. *Electrohydrodynamics: Basic Concepts, Problems and Applications* (Kursk: Technical Univ. Press, 1996)
21. Korolev Yu D, Mesyats G A. *Avtomissionnye i Vzryvnye Protsessy v Gazovom Razryade* (Autoemissive and Explosive Processes in Gas Discharge) (Novosibirsk: Nauka, 1982)
22. Malter L. *Phys. Rev.* **50** 48 (1936)
23. Kaminsky M. *Atomic and Ionic Impact Phenomena on Metal Surfaces* (New York: Academic Press, 1965) [Translated into Russian (Moscow: Mir, 1967)]
24. *Elektronnaya Emissiya* (Electronic Emission) (Moscow: IL, 1962)
25. Brouche M, Gosse Y-P, in *Proc. of 1996 IEEE 12th Intern. Conf. on Conduction and Breakdown in Dielectric Liquids, Rome, Italy, July 15–19, 1996* (New York: IEEE, 1996) p. 130
26. Basseches H, Barres M W. *Ind. Eng. Chem.* **50** 959 (1958)
27. Mesyats G A. *Usp. Fiz. Nauk* **165** 601 (1995) [*Phys. Usp.* **38** 567 (1995)]
28. Little R P, Whitney W T J. *Appl. Phys.* **34** 2430 (1963)
29. Ostroumov G A. *Vzaimodeistvie Elektricheskikh i Elektrogidrodinamicheskikh Polei: Fizicheskie Osnovy Elektrodinamiki* (Interaction of Electric and Electrohydrodynamic Fields: Physical Foundation of Electrodynamics) (Moscow: Nauka, 1979)
30. Rubashov I B, Bortnikov Yu S. *Elektrogazodinamika* (Electrogas-dynamics) (Moscow: Atomizdat, 1971)
31. Zhakin A I, Tarapov I E, Fedonenko A I. *Elektronnaya Obrabotka Materialov* (5) 37 (1983)
32. Zhakin A I, in *Electrohydrodynamics* (CISM Courses and Lectures, No. 380, Ed. A Castellanos) (Wien: Springer, 1998) p. 83
33. Lacroix J C, Atten P, Hopfinger E J J. *Fluid Mech.* **69** 539 (1975)

34. Kiselev V F, Kozlov S N, Zoteev A V *Osnovy Fiziki Poverkhnosti Tverdogo Tela* (Fundamentals of Solid Surface Physics) (Moscow: Nauka, 1999)
35. Zhakin A I *Izv. Akad. Nauk SSSR, Mekh. Zhidkosti Gaza* (4) 3 (1986)
36. Felici N J, Gosse J P *Revue Phys. Appl.* **14** 629 (1979)
37. Stishkov Yu K, Ostapenko A A *Elektrogidrodinamicheskie Tsecheniya v Zhidkikh Dielektrikakh* (Electrohydrodynamic Flows in Liquid Dielectrics) (Leningrad: Izd. LGU, 1989)
38. Thomson J J (Sir), Thomson G P *Conduction of Electricity Through Gases* Vol. 1, 3rd ed. (Cambridge: Univ. Press, 1928) p. 193
39. Semenikhin N M, Zholkovskii E K *Elektrokhimiya* **18** 691 (1982)
40. Semenikhin N M, Zholkovskii E K *Elektrokhimiya* **18** 874 (1982)
41. Semenikhin N M, Zholkovskii E K *Elektrokhimiya* **18** 1323 (1982)
42. Rychkov Yu M, Stishkov Yu K *Kolloidn. Zh.* **6** 1204 (1978)
43. Zhakin A I *Elektronnaya Obrabotka Materialov* (2) 48 (1988)
44. Morrison S R *The Chemical Physics of Surfaces* (New York: Plenum Press, 1977) [Translated into Russian (Moscow: Mir, 1980)]
45. Vol'kenshtein F F *Elektronnyye Protsestry na Poverkhnosti Poluprovodnikov pri Khemosorbtsii* (Electronic Processes on Semiconductor Surfaces Under Chemical Sorption) (Moscow: Nauka, 1987) [Translated into English (New York: Consultants Bureau, 1991)]
46. Frumkin A N *Elektrodnye Protsestry. Izbrannye Trudy* (Electrode Processes. Selected Works) (Moscow: Nauka, 1987)
47. Damaskin B B, Petrii O A *Vvedenie v Elektrokhimicheskuyu Kinetiku* (Introduction to Electrochemical Kinetics) 2nd ed. (Moscow: Vysshaya Shkola, 1983)
48. Bagotzky V S *Osnovy Elektrokhimii* (Fundamentals of Electrochemistry) (Moscow: Khimiya, 1988) [Translated into English (New York: Plenum Press, 1993)]
49. Krishtalik L I *Elektrodnye Reaktsii. Mekhanizm Elementarnogo Akta* (Electrode Reactions. Mechanism of Elementary Act) (Moscow: Nauka, 1979) [Translated into English: *Charge Transfer Reactions in Electrochemical and Chemical Processes* (New York: Consultants Bureau, 1986)]
50. Dogonadze R R, Krishtalik L I *Usp. Khim.* **44** 1987 (1975) [*Russ. Chem. Rev.* **44** 938 (1975)]
51. Dogonadze R R, Kuznetsov A M "Sovremennoe sostoyanie teorii elektrodnykh protsessov" ("Modern theory of electrode processes") in *Itogi Nauki. Ser. Elektrokhimiya 1967* (Progress in Science. Ser. Electrochemistry 1967) (Moscow: VINITI, 1969) p. 5
52. Goronovskii I T, Nazarenko Yu P, Nekryach E F *Kratkii Spravochnik po Khimii* (Concise Reference Book on Chemistry) (Ed. A T Pilipenko) 5th ed. (Kiev: Naukova Dumka, 1987)
53. Zakharchenko V V et al. *Elektrizatsiya Zhidkosti i ee Predotvrashchenie* (Electrization of Liquids and Its Prevention) (Moscow: Khimiya, 1976)
54. Bobrovskii S A, Yakovlev E I *Zashchita ot Staticheskogo Elektrichstva v Neftyanoi Promyshlennosti* (Protection from Static Electricity in Oil Industry) (Moscow: Nedra, 1983)
55. Koszman I, Gavis J *Chem. Eng. Sci.* **17** 1023 (1962)
56. Gavis J, Koszman I J *Colloid Sci.* **16** 375 (1961)
57. Fridrikhsberg D A, Shchiglovskii N V, in *Issledovaniya v Oblasti Poverkhnostnykh Sil* (Surface Forces Research) (Moscow: Nauka, 1967) p. 421
58. Gogosov V V, Nikiforovich E N, Tolmachev V V *Magnitnaya Gidrodinamika* (2) 59 (1979)
59. Zhakin A I *Priklad. Mekh. Tekh. Fiz.* (5) 31 (1982)
60. Delahay P *New Instrumental Methods in Electrochemistry: Theory, Instrumentation, and Applications to Analytical and Physics Chemistry* (New York: Interscience Publ., 1954) [Translated into Russian (Moscow: IL, 1957)]
61. Swan D W, Lewis T J *Proc. Phys. Soc. London* **73** 501 (1961)
62. Swan D W, Lewis T J *J. Electrochem. Soc.* **107** 180 (1960)
63. Sletten A M *Nature* **183** 311 (1957)
64. Green W B J. *Appl. Phys.* **26** 1257 (1955)
65. Preston G P, Bircumshaw L L *Philos. Mag.* **7** 707 (1935)
66. Zhakin A I *Magnitnaya Gidrodinamika* (2) 70 (1982)
67. Maissel L I, Glang R (Eds) *Handbook on Thin Film Technology* (New York: McGraw-Hill, 1970) [Translated into Russian: Vol. 2 (Moscow: Sovetskoe Radio, 1977)]
68. Mott N F, Gurney R W *Electronic Processes in Ionic Crystals* 2nd ed. (Oxford: Clarendon Press, 1948) Ch. V
69. Kaptsov N A *Koronnyi Razryad* (Corona Discharge) (Moscow: Gostekhizdat, 1947)
70. Vatazhin A B et al. *Elektrogazodinamicheskie Tsecheniya* (Electro-gazodynamic Flows) (Ed. A B Vatazhin) (Moscow: Nauka, 1983)
71. Halpern B, Gomer R J. *Chem. Phys.* **43** 1069 (1965)
72. Halpern B, Gomer R J. *Chem. Phys.* **51** 1031 (1969)
73. Smirnov B M *Fizika Slaboionizovannogo Gaza v Zadachakh s Resheniyami* (Physics of Weakly Ionized Gas in Problems with Solutions) 3rd ed. (Moscow: Nauka, 1985) [Translated into English: *Physics of Weakly Ionized Gases (Problems and Solutions)* (Moscow: Mir Publ., 1981)]
74. Biberman L M, Vorob'ev V S, Yakubov I T *Kinetika Neravnovesnoi Nizkoterturnoi Plazmy* (Kinetics of Non-Equilibrium Low-Temperature Plasmas) (Moscow: Nauka, 1982) [Translated into English (New York: Consultants Bureau, 1987)]
75. Sinkevich O A, Stakhanov I P *Fizika Plazmy. Statsionarnyye Protsestry v Chastichno Ionizovannom Gaze* (Plasma Physics. Stationary Processes in Partially Ionized Gas) (Moscow: Vysshaya Shkola, 1991)
76. Rose A *Phys. Rev.* **97** 1538 (1955)
77. Shikin V B, Monarkha Yu P *Dvumernyye Zaryazhennyye Sistemy v Gelii* (Two-Dimensional Charged Systems in Helium) (Moscow: Nauka, 1989)
78. Stern F "Quantum properties of surface space-charge layers" *Crit. Rev. Solid State Sci.* **5** 499 (1974) [Translated into Russian: in *Novoe v Issledovanii Poverkhnosti Tverdogo Tela* (News in Solid Surface Research) Issue 2 (Moscow: Mir, 1977)]
79. Volkov V A, Petrov V A, Sandomirskii V B *Usp. Fiz. Nauk* **131** 423 (1980) [*Sov. Phys. Usp.* **23** 375 (1980)]
80. Ando T, Fowler A B, Stern F *Rev. Mod. Phys.* **54** 437 (1982)
81. Komnik Yu F *Fizika Metallicheskiy Plenok: Razmernyye i Strukturnyye Effekty* (Metal Film Physics: Dimensional and Structural Effects) (Moscow: Atomizdat, 1979)
82. Partenskii N B *Usp. Fiz. Nauk* **128** 69 (1979) [*Sov. Phys. Usp.* **22** 330 (1979)]
83. Ansel'm A I *Vvedenie v Teoriyu Poluprovodnikov* (Introduction to Semiconductor Theory) 2nd ed. (Moscow: Nauka, 1978) [Translated into English (Moscow: Mir, 1981)]
84. Boudreaux D S, Cutler P H *Surf. Sci.* **5** 230 (1966)
85. Smirnova N A *Metody Statisticheskoi Termodinamiki v Fizicheskoi Khimii* (Methods of Statistical Thermodynamics in Physical Chemistry) (Moscow: Vysshaya Shkola, 1973)
86. Davydov A S *Kvantovaya Mekhanika* (Quantum Mechanics) (Moscow: Fizmatlit, 1963) [Translated into English (Oxford: Pergamon Press, 1965)]
87. Blokhintsev D I *Osnovy Kvantovoi Mekhaniki* (Fundamentals of Quantum Mechanics) (Moscow: Nauka, 1976)
88. Smirnov B M *Otritsatel'nye Iony* (Negative Ions) (Moscow: Atomizdat, 1978) [Translated into English (New York: McGraw-Hill, 1982)]
89. Vedenev V I et al. *Energiya Razryva Khimicheskikh Svyazei, Potentsialy Ionizatsii i Srodstvo k Elektronu: Spravochnik* (Bond Rupture Energies, Ionization Potentials, and Electron Affinities: Reference Book) (Moscow: Izd. AN SSSR, 1962)
90. Radchenko I V *Molekulyarnaya Fizika* (Molecular Physics) (Moscow: Nauka, 1965)
91. Kopylov Yu A *Trudy Dnepropetrovskogo Sel'skokhozyaistvennogo Inst. Organicheskie Poluprovodn.* **27** 3 (1974)
92. Artana G et al., in *Proc. of 1996 IEEE 12th Intern. Conf. on Conduction and Breakdown in Dielectric Liquids, Rome, Italy, July 15–19, 1996* (New York: IEEE, 1996) p. 137
93. Dikarev B et al., in *Proc. of 1999 IEEE 13th Intern. Conf. on Conduction and Breakdown in Dielectric Liquids, Nara, Japan, July 20–25, 1999* (Nava-Ken: New Public Hall, 1999) p. 33
94. Sazhin V I, Shuvaev V P *Elektrokhimiya* **2** 831 (1966)
95. Bologa M K, Grosu F P, Kozhukhar' I A, in *Elektrokonveksiya i Teploobmen* (Electroconvection and Heat Exchange) (Ed. G A Ostroiov) (Kishinev: Shtiintsa, 1977)
96. Jones T B *Adv. Heat Transf.* **14** 107 (1978)
97. Melcher J *Magnitnaya Gidrodinamika* (2) 3 (1974)
98. Melcher J R, Taylor G I "Electrodynamic: A review of the role of interfacial shear stresses" *Annu. Rev. Fluid Mech.* **1** 111 (1969) [Translated into Russian: in *Mekhanika. Periodicheskii Sbornik Perevodov Inostrannykh Statei* (Moscow: Mir, 1971) p. 68]